

Level-statistics in Disordered Systems: A single parametric scaling and Connection to Brownian Ensembles

Pragya Shukla*

(i) Department of Physics, Indian Institute of Technology, Kharagpur-721302, India,
(ii) Max-Planck Institute for Physics of Complex Systems, Nothnitzer Str.38, Dresden-01187, Germany.
(February 8, 2020)

We find that the statistics of levels undergoing metal-insulator transition in systems with multi-parametric Gaussian disorders and non-interacting electrons behaves in a way similar to that of the single parametric Brownian ensembles [1]. The latter appear during a Poisson \rightarrow Wigner-Dyson transition, driven by a random perturbation. The analogy provides the analytical evidence for the single parameter scaling of the level-correlations in disordered systems as well as a tool to obtain them at the critical point for a wide range of disorders.

PACS numbers: 05.45+b, 03.65 sq, 05.40+j

The spectral correlations of a disordered system are very sensitive to the behavior of its eigenfunctions. The presence of disorder may cause localized waves in the system, implying lack of interaction between certain parts. This is reflected in the structure of the Hamiltonian matrix which is sparse or banded in the site representation depending on dimensionality of the system. The variation of the disorder-strength can lead to a metal-insulator transition (MIT), with eigenfunctions changing from a fully extended state (metal) to a strongly localized one (insulator) with partial localization in the critical region. The associated Hamiltonian also undergoes a transition, *in effect*, from a full matrix to a sparse or banded form and finally to a diagonal matrix. The statistical studies of levels for various degrees and types of disorders require, therefore, analysis of different ensembles. Here the nature of the localization and its strength is reflected in the measure and the sparsity of the ensemble, respectively. Our objective in this paper is to obtain a mathematical formulation for the level-correlations, common to a large class of disorders (Gaussian type); the information about the nature of disorder enters in the formulation through a parameter, basically a function of various parameters influencing the localization.

Recently it was shown that the eigenvalue distributions of various ensembles, with a multi-parametric Gaussian measure and independent matrix elements, appear as non-equilibrium stages of a Brownian type diffusion process [2]. Here the eigenvalues evolve with respect to a single parameter which is a function of the distribution parameters of the ensemble. The parameter is therefore related to the complexity of the system represented by the ensemble and can be termed as the "complexity" parameter. The solution of the diffusion equation for a given value of the complexity parameter gives the distribution of the eigenvalues, and thereby their correlations, for the corresponding system. A similar diffusion equa-

tion is known to govern the evolution of the eigenvalues of Brownian Ensembles (BE) [1,3,6] and many of its solutions for various initial conditions have already been obtained [7]. The analogy can then be used to obtain the level-correlations for the Gaussian random matrix models of the disordered systems with non-interacting electrons. The presence of interactions introduces a correlation between matrix elements of the ensemble representing the system; the details of this case will be discussed elsewhere.

The correlations in the single electron spectra of disordered metals are governed by a variety of parameters e.g the associated energy-ranges, degree of disorder, the dimensionality of the system etc. Here the two energy-scales, playing the dominant role, are the Thouless energy E_c and the mean level spacing Δ . The E_c is given by the time-scale needed by the wave-packet to diffuse through the sample. In the diffusive (metallic) regime and for energy-scales δE smaller than E_c , the spectral correlations are well-modeled by Wigner-Dyson (WD) ensembles [3,6]. For $\delta E > E_c$, the statistics deviate from the Wigner-Dyson case, however the deviations are negligible for sample size $L \rightarrow \infty$. In the localized (insulator) phase too, the correlations are energy-dependent but, in the limit $L \rightarrow \infty$, the levels are completely uncorrelated and their statistics can be modeled by the Poisson ensemble. However the statistics in the critical region near the metal-insulator transition (Anderson type) is different from both Wigner-Dyson as well as Poisson statistics and depends on various system dependent features [4,5]. Our study shows that the multi-parametric level-statistics in the critical region can be well-modeled by the single-parametric Brownian Ensembles.

The paper is organized as follows. The section I contains a brief description of the simplest model of a disordered system using independent electron approximation and the equation governing the evolution of its eigenval-

ues due to change of disorder etc. The properties of the BEs useful for present study are given in section II. The section III deals with the determination of the single parameter Λ governing the level-statistics during MIT using BE-analogy. It also explains, in terms of Λ , some of the already known features of the statistics. This provides an analytical support to use the BEs to obtain the unknown spectral fluctuations during MIT, given in section IV. The section V contains the details of the numerical comparison of the level-statistics of Anderson Hamiltonian with that of BEs and reconfirms our analytical results.

I. THE MULTI-DIMENSIONAL ANDERSON HAMILTONIAN

The Anderson model for a disordered system is described by a d -dimensional disordered lattice, of size L , with a Hamiltonian $H = \sum_n \epsilon_n a_n^+ a_n - \sum_{n \neq m} b_{mn} (a_n^+ a_m + a_n a_m^+)$ in tight-binding approximation. The site energies ϵ_n , measured in units of the overlap integral between adjacent sites, correspond to the random potential. The hopping is assumed to connect only the z nearest-neighbors (referred by m) of each site. In the site representation, H turns out to be a sparse matrix of size $N = L^d$ with diagonal matrix elements as the site energies $H_{kk} = \epsilon_k$. The off-diagonals H_{kl} describe the interaction between two sites k and l ; here H_{kl} for two sites connected by hopping will be referred as hopping off-diagonal and the rest as non-hopping off-diagonals. The level-statistics of H can therefore be studied by analyzing the properties of an ensemble of (i) sparse real symmetric matrices, in presence of a time-reversal symmetry and (ii) sparse complex Hermitian matrices in absence of a time-reversal.

We consider an ensemble of Anderson Hamiltonians (later referred as Anderson ensemble) with a Gaussian type disorder. The site-energies $H_{kk} = \epsilon_k$ are thus independent Gaussian distributions $\rho_{kk}(H_{kk}) = e^{-(H_{kk} - b_{kk})^2/2h_{kk}}$ with variance h_{kk} and mean b_{kk} . The hopping can be chosen to be isotropic or anisotropic, non-random or random (Gaussian). A general form of the probability density $\rho(H) \equiv \prod_{k,l;k \leq l} \rho_{kl}(H_{kl})$ of the ensemble, including all the above possibilities, can therefore be given by

$$\rho(H, h, b) = C \exp\left[-\sum_{s=1}^{\beta} \sum_{k \leq l} (1/2h_{kl;s})(H_{kl;s} - b_{kl;s})^2\right] \quad (1)$$

with subscript "s" of a variable referring to its components, β as their total number ($\beta = 1$ for real variable, $\beta = 2$ for the complex one), C as the normalization constant, h as the set of the variances $h_{kl;s} = \langle H_{kl;s}^2 \rangle$ and b as the set of all mean values $\langle H_{kl;s} \rangle = b_{kl;s}$. As obvious, in the limit $h_{kl;1}, h_{kl;2} \rightarrow 0$, eq.(1) corresponds to the non-random nature of H_{kl} (that is,

$\rho_{kl}(H_{kl}) = \delta(H_{kl} - b_{kl})$). Note although the non-hopping off-diagonals in Anderson matrix always remain zero but the effective sparsity of the matrix changes due to change in relative strength of the diagonals and the hopping off-diagonals. Thus, in the insulator limit (with almost no overlap between site energies due to strong disorder), the matrix behaves effectively as a diagonal one, the diagonals being very large as compared to hopping off-diagonals. In the opposite limit of very weak disorder when an average diagonal is nearly of the same strength as an average off-diagonal, the statistical behavior of the matrix is same as that of a matrix taken from a Wigner-Dyson ensemble [3]. The latter are the basis-invariant Gaussian ensembles of Hermitian type, with a same variance for almost all matrix elements. The statistical behavior of levels in the Wigner-Dyson ensembles depends only on their symmetry class and is therefore universal in nature. The three main universality classes are described by a parameter β , basically a measure of the degree of level-repulsion [3,6]: (i) GOE with $\beta = 1$, corresponding to time-reversal symmetry and integer angular momentum, (ii) GUE with $\beta = 2$ and no time-reversal symmetry, (iii) GSE with $\beta = 4$ and time-reversal symmetry but half integer angular momentum.

A variation of disorder and hopping rate changes the distribution parameters of the probability density $\rho(H)$ and thereby its statistical properties. Using Gaussian nature of ρ , it is easy to verify that under a change of parameters $h_{kl} \rightarrow h_{kl} + \delta h_{kl}$ and $b_{kl} \rightarrow b_{kl} + \delta b_{kl}$, the matrix elements H_{kl} undergo a diffusion dynamics along with a finite drift,

$$\begin{aligned} \sum_{k \leq l;s} \left[(2/\tilde{g}_{kl}) x_{kl;s} \frac{\partial \rho}{\partial h_{kl;s}} - \gamma b_{kl;s} \frac{\partial \rho}{\partial b_{kl;s}} \right] = \\ \sum_{kl;s} \frac{\partial}{\partial H_{kl;s}} \left[\frac{g_{kl}}{2} \frac{\partial}{\partial H_{kl;s}} + \gamma H_{kl;s} \right] \rho \end{aligned} \quad (2)$$

where $x_{kl;s} \equiv 1 - \gamma \tilde{g}_{kl} h_{kl;s}$ with $\tilde{g}_{kl} = 2 - \delta_{kl}$ and $g_{kl} = 1 + \delta_{kl}$. The γ is an arbitrary parameter, giving the variance of the matrix elements at the end of the evolution [2]. The above equation describes a multi parametric flow of matrix elements from an arbitrary initial condition, say H_0 . However, as discussed in [2], it is possible to define a "complexity" parameter Y , a function of various distribution parameters $h_{kl;s}$ and $b_{kl;s}$, in terms of which the matrix elements undergo a single parametric diffusion,

$$\frac{\partial \rho}{\partial Y} = \sum_{kl;s} \frac{\partial}{\partial H_{kl;s}} \left[\frac{g_{kl}}{2} \frac{\partial}{\partial H_{kl;s}} + \gamma H_{kl;s} \right] \rho \quad (3)$$

with

$$Y = -\frac{1}{2M\gamma} \ln \left[\prod_{k \leq l} \prod_{s=1}^{\beta} |x_{kl;s}| \cdot |b_{kl;s}|^2 \right] + C \quad (4)$$

here \prod' implies a product over non-zero $b_{kl;s}$ and $x_{kl;s}$. Further, C is a constant determined by the initial distribution, M is the number of all non-zero parameters $x_{kl;s}$ and $b_{kl;s}$ and $\beta = 1, 2$ for Hamiltonians with and without time-reversal, respectively.

The solution of the eq.(3) gives the state $\rho(H, Y|H_0, Y_0)$ of the flow at parameter value Y , starting from an initial state H_0 with $Y = Y_0$. An integration over initial probability density result in the density given by eq.(1) in terms of $Y(h, b)$: $\rho(H, Y) = \int \rho(H, Y|H_0, Y_0)\rho(H_0, y_0)dH_0$. The evolution reaches a steady state when $\partial\rho/\partial Y \rightarrow 0$ with the ensemble $\rho(H)$ approaching the Wigner-Dyson limit, $\rho \propto e^{-(\gamma/2)\text{Tr}H^2}$.

As implied by eq.(3), the distribution $\rho(H|H_0)$, depends on the multiple parameters h_{kl} , b_{kl} (for all k, l) only through a function Y , that is, $P(H, h, b|H_0) \equiv P(H, Y(h, b)|H_0)$. This can be proved by considering a transformation of the M non-zero variables of the sets h and b to another set $\{Y, Y_2, \dots, Y_M\}$ of M variables; $h_{kl} = h_{kl}(Y, Y_2, \dots, Y_M)$ and $b_{kl} = b_{kl}(Y, Y_2, \dots, Y_M)$. As shown in [2], it is possible to define Y, Y_2, \dots, Y_M such that the $M-1$ variables Y_2, \dots, Y_M remain constant during the evolution of P due to any change in sets h, b . The statistics during the transition is therefore governed by Y only. The choice of the Y_2, \dots, Y_M depends on the system under consideration. For a transition preserving the lattice structure, these constants turn out to be the functions of the site-indices in the lattice. For example, the variances h_{kl} in the Anderson ensemble are functions of the disorder as well as the site-indices k, l ; Y can then be identified as a function of disorder while Y_j ($j > 1$) as the functions of site indices. Further, as these constants do not appear in eq.(3), its solution and therefore the ensemble-statistics is independent of the specific values of the constants.

The flow described by eq.(3) can start from any initial state; the only constraint on the choice is that the parameters Y_j for the initial ensemble should be same as those for the ensemble $\rho(H, y, b)$. As shown below by an example, the initial state can also be chosen as the insulator limit of the disordered system, described by an ensemble of diagonal matrices. Although this corresponds to a same value for all initial off-diagonal variances (that is, zero), however a choice of different rates of change of h_{kl} with respect to Y can result in different possible values for each h_{kl} at a later stage.

As an example, consider an Anderson system with a Gaussian site disorder (of variance $W^2/12$ and mean zero), same for each site, and an isotropic Gaussian hopping with a non-random component (of variance $W_s^2/12$ and mean t_s with $s = 1, 2$ for real and imaginary parts respectively) between nearest neighbors (referred as ensemble "G" later on). The corresponding probability density can be described by eq.(1) with $h_{kk} = W^2/12$, $b_{kk} = 0$ and $h_{kl;s} = f_1(kl; s)$, $W_s^2/12$, $b_{kl;s} = f_2(kl; s)$, t_s where

$f_1(kl; s) = 1$, $f_2(kl; s) = 1$ for for $\{k, l\}$ pairs representing hopping, $f_1(kl; s) \rightarrow 0$ and $f_2(kl; s) \rightarrow 0$ for all $\{k, l\}$ values corresponding to disconnected sites. As obvious, here the distribution parameters h_{kl} depend on more than one system parameters, namely, the disorder parameters W , W_1 and W_2 as well as various functions of site-indices. The latter, being invariant of motion, give the parameters Y_2, \dots, Y_M . The Y for this case can be obtained by using eq.(4),

$$Y = -\frac{N}{2M\gamma}\alpha + C \quad (5)$$

$$\alpha = \ln|1 - \gamma W^2/12| + (z/2) \sum_s \ln [|1 - \gamma W_s^2/6| |t_s + \delta_{t_s 0}|] + C, \quad (6)$$

with $M = \beta N(N + z(1 - \delta_{t_0}) + 2 - \beta)/2 \approx \beta N^{2+\epsilon}/2$. Here zN is the number of connected sites (nearest-neighbors) which depends on the topology and the dimensionality d of the system and the ϵ is a function of z , $\epsilon(z) = (\log(N + z(1 - \delta_{t_0}) + 2 - \beta)/\log N) - 1$; $\epsilon \rightarrow 0$ for $z \ll N$.

Now consider an insulator as the initial state (in the same site-basis as used for "G") with zero hopping, that is, $W_s = 0$, $t_s = 0$ and a Gaussian site disorder with variance $(W^2/12) = (2\gamma)^{-1}$ (referred as "G₀"). As obvious, this corresponds to an ensemble of diagonal matrices with $h_{kk} = (2\gamma)^{-1}$, $h_{kl;s} = 0$ for $k \neq l$ and $b_{kl;s} = 0$ for all k, l . A substitution of these values in eq.(5) gives the initial value of Y , say Y_0 , where $Y_0 = -\frac{N}{2\gamma M}\alpha_0 + C$ with $\alpha_0 = -\ln 2$. Note, the basis being same, the parameters Y_j (for $j \geq 2$) are same for both G and G_0 . (The advantage of choosing the above initial state is explained later). As obvious, starting from G_0 , a variation of diagonal disorder W , hopping parameters W_s and t_s with rates $\delta h_{kk}/\delta W = W/6$, $\delta h_{kl;s}/\delta W_s = W_s f_1(kl; s)/6$ and $\delta b_{kl;s}/\delta t_s = t_s f_2(kl; s)$ for $k \neq l$, respectively, can lead to the ensemble G . Using $(\partial Y_j/\partial x) = 0$ for $j \geq 2$ with $x \equiv W, W_s, t_s$, and, eq.(5) to obtain $(\partial Y/\partial x)$, it can be seen that the above rates correspond to $\frac{\partial h_{kk}}{\partial Y} \propto |1 - \gamma W^2/12|$, $\frac{\partial h_{kl}}{\partial Y} \propto f_1|1 - \gamma W_s^2/6|$ and $\frac{\partial b_{kl}}{\partial Y} \propto f_2 t_s$; the variances and means of different matrix elements therefore change with different rates with Y .

The distribution P of the eigenvalues E_n for a metal (for the energy ranges with fully extended eigenfunctions) is given by the Wigner-Dyson distribution, $P(\{E_n\}) = \prod_{i < j} |E_i - E_j|^\beta e^{-\frac{\gamma}{2} \sum_k E_k^2}$, and, for an insulator by a Poisson distribution [4]. The distribution for various transition stages can be obtained by integrating ρ over the associated eigenvector space. Let $P(\{E_n\}, h, b)$ be the joint probability of finding eigenvalues λ_i of H between E_i and $E_i + dE_i$ ($i = 1, 2, \dots, N$) at a given h and b , it can then be expressed as $P(\{E_n\}, h, b) = \int \prod_{i=1}^N \delta(E_i - \lambda_i) \rho(H, h, b) dH$. Using the above definition in eq.(3), it can be shown that the eigenvalues of $\rho(H)$

undergo a diffusion dynamics along with a finite drift due to their mutual repulsion, (see [2] also)

$$\frac{\partial P}{\partial Y} = \sum_n \frac{\partial}{\partial E_n} \left[\frac{\partial}{\partial E_n} + \sum_{m \neq n} \frac{\beta}{E_m - E_n} + \gamma E_n \right] P \quad (7)$$

Again the steady state of the evolution is given by the limit $\partial P/\partial Y \rightarrow 0$; $P(\{E_n\})$ in this limit turns out to be a Wigner-Dyson distribution.

The eq.(7) can be used to obtain the correlations between levels. For example, a knowledge of its solution P gives the static correlations

$$R_n(E_1, E_2, \dots, E_n; Y) = \frac{N!}{(N-n)!} \int P(\{E_j\}, Y) dE_{n+1} \dots dE_N$$

The P can be obtained by using the analogy of eq.(7) with the equation governing the evolution of the eigenvalues of Brownian ensembles (BE) of hermitian type [1,3]. The latter, has been studied in great detail in past and many of its statistical spectral properties are already known [7]. A brief description of the BE is given in the next section.

It should be noted here that the single-parametric evolution of the matrix elements of the AE in terms of the complexity parameter $Y - Y_0$ would result in a similar evolution for their eigenvector components too; this can be shown by integrating the eq.(3) over all eigenvalues. However in this paper we confine ourselves to the discussion of eigenvalue statistics only; the details for the eigenvector statistics will be published elsewhere.

II. SPECTRAL PROPERTIES OF BROWNIAN ENSEMBLES

A Brownian ensemble corresponds to a non-stationary state of the matrix elements undergoing a transition due to a random perturbation of a stationary ensembles by another stationary ensembles. The nature of a BE, appearing during the transition, depends on the stationary ensembles. Based on the underlying symmetry, the latter can be of various types and the transitions between their different pairs may give rise to different BEs; see [3,6] for detail. Here we discuss only the BEs appearing during a transition from Poisson \rightarrow Wigner-Dyson ensemble (referred as Wigner-Dyson transition or WDT) caused by a perturbation of the former by the latter. As this transition results in a change of localized eigenstates to delocalized ones, its relevance for the study of MIT is intuitively suggested.

The BEs related to the Poisson \rightarrow Wigner-Dyson transition can be described by a $N \times N$ ensemble $H = \sqrt{f}(H_0 + \lambda V)$ (with $f = (1 - \lambda^2)^{-1}$). Here V is a random perturbation of strength λ , taken from a Wigner-Dyson ensemble, and applied to an initial stationary state H_0

given by a Poisson ensemble of diagonal matrices. The ensemble H can thus be represented by the following probability distribution for all (independent) matrix elements:

$$\rho(H) \propto \exp \left[-\gamma \sum_{i=1}^N H_{ii}^2 - 2\gamma(1+\mu) \sum_{i < j} |H_{ij}|^2 \right] \quad (9)$$

with $(1+\mu) = (\lambda^2 f)^{-1}$; here $H = H_0$ for $\lambda \rightarrow 0$ or $\mu \rightarrow \infty$. An ensemble H given by the above measure, is also known as Rosenzweig-Porter ensemble (RPE); Note it also corresponds to an ensemble of Anderson Hamiltonians with very long range, isotropic, random hopping.

The eq.(7) describes the evolution of the eigenvalues of a generalized Gaussian ensemble with a probability density (1) and is therefore applicable for the BEs defined by a probability density (9) too. A comparison of measure (9) with measure (1), gives a variance $h_{kl;s} = (4\gamma(1+\mu))^{-1}$, $h_{kk;s} = (2\gamma)^{-1}$ and mean $b_{kl;s} = 0$ for all k, l and s indices. Using these values in eq.(4), the parameter Y for the BE case can be given as

$$\begin{aligned} Y &= -\frac{1}{2\gamma} \frac{(N-1)}{(N+2-\beta)} \log \left(1 - \frac{1}{2(1+\mu)} \right) + Y_0 \\ &\approx \frac{1}{4\gamma\mu} + Y_0 \quad (\text{for } \mu \gg 1) \end{aligned} \quad (10)$$

with $M = \beta N(N+2-\beta)/2$ and $Y_0 = \frac{N}{2\gamma M} \ln 2 + C$ as the complexity parameter of the ensemble H_0 (note, $Y = Y_0$ for $\mu \rightarrow \infty$).

A typical matrix in the ensemble (9) has the diagonal elements of order $\gamma^{-1/2}$ and off-diagonals of the order of $(\gamma\mu)^{-1/2} (= o(Y - Y_0)^{1/2})$. The number of off-diagonals being N times more than the diagonals, the matrix behavior is governed by the parameter μ . Thus, for large BE ($N \rightarrow \infty$), a radical change from Wigner-Dyson case can only occur if μ increases more rapidly than N (which makes the total strength of the off-diagonals weaker than that of diagonals). This results in three different regimes of the mean-level density $R_1(E)$ [8]:

$$R_1(E) = \frac{N}{\sqrt{\pi}} e^{-E^2} \quad \text{for } N(Y - Y_0) \rightarrow 0 \quad (11)$$

$$= \frac{\sqrt{8N\gamma(Y - Y_0) - E^2}}{4\gamma\pi(Y - Y_0)} \quad \text{for } N(Y - Y_0) \rightarrow \infty \quad (12)$$

$$= NF(E, a) \quad \text{for } N(Y - Y_0) = a \quad (13)$$

with a as an N -independent constant. Although the exact form of the function $F(E, a)$ is not known, its limiting behavior can be given as follows: $F(E, a) \approx e^{-E^2}/\sqrt{\pi}$ for $a \ll 1$ and $F(E, a) \approx (4\pi\gamma a)^{-1} \sqrt{8\gamma a - E^2}$ for $a \gg 1, E^2 \ll a$ [8].

The mean level density changes from an exponential to semi-circular form at the scale of $N(Y - Y_0)$; its evolution can therefore be described in terms of the parameter

$(Y - Y_0)$. The same is not true for the R_n , $n > 1$. This is because the correlation between levels is governed by the strength ($\approx o(N^2|Y - Y_0|^{1/2})$) of the off-diagonals relative to the diagonals (strength $\approx o(N)$). As a result, their transition to equilibrium, with $|Y - Y_0|$ as the evolution parameter, is rapid, discontinuous for infinite dimensions of matrices [1]. But for small- Y and large N , a smooth crossover can be seen in terms of a rescaled parameter $\Lambda(E)$:

$$\Lambda(E) = |Y - Y_0|/\Delta_\eta^2 \quad (14)$$

with $\Delta_\eta(E, Y) = \Delta N/\eta$ as the mean-level spacing in the correlated region of the spectrum, $\eta \equiv \eta(E, Y)$ as the correlated "volume" and the $\Delta \equiv \Delta(E, Y) = R_1^{-1}$ as the mean level spacing of the whole spectrum at energy E and the parameter $Y - Y_0$. The correlation volume η is a measure of the degree of localization of the eigenfunctions and can be determined by a knowledge of the inverse participation ratio I_2 ; $\eta \propto (I_2)^{-1}$. For finite N , Δ_η varies smoothly with changing μ which results in a continuous family of BEs, parameterized by Λ , existing between Poisson and Wigner-Dyson limit. However the level-statistics for the large BE ($N \rightarrow \infty$) can be divided into three regions [8]:

(i) **Poisson regime:** $N^2(Y - Y_0) \rightarrow 0$: The off-diagonals, responsible for the correlation between levels, are negligible which results in a very small correlation volume $\eta \ll N$. The lack of repulsion between levels results in a mean level spacing $\Delta \propto N^{-1}$ (see eq.(11)), thereby, giving $\Lambda \rightarrow 0$ and the Poisson statistics,

(ii) **WD regime:** $N^2(Y - Y_0) \rightarrow \infty$: The contribution from both, the diagonals as well as off-diagonals is of the same order, leading to long-range correlations between levels and an increased correlation volume $\eta > N$. The repulsion of levels now results in an increased mean level spacing $\Delta \propto N^{-1/2}$. (see eqs.(12,13)) which gives $\Lambda \rightarrow \infty$ and Wigner-Dyson statistics.

(iii) **Critical regime:** $N^2(Y - Y_0) = (4\gamma c)^{-1}$ = a constant: For $\mu = cN^2$ with c as a constant independent of N , a sequence of approximately $o(1/\sqrt{c})$ levels show Wigner-Dyson behavior. The more distant levels display weak correlations of the type existing near the Poisson limit resulting in a $\Delta \approx o(1/N)$. However the interaction between levels, although weak, is spread in the entire spectrum which gives $\eta \approx N$. The parameter Λ is therefore N -independent: $\Lambda(E) = (1/4c\pi\gamma)e^{-E^2}$; note it is also independent of the symmetry parameter β .

The finite, non-zero Λ -value for $\mu = cN^2$ in limit $N \rightarrow \infty$ therefore gives rise to a third statistics, intermediate between Poisson and Wigner-Dyson ensemble, which is known as the critical Brownian ensemble (CBE). This being the case for arbitrary values of c (non-zero and finite), an infinite family of critical BE, characterized by c (or $\mu_c = cN^2$), occurs during WDT. The presence of such a family can be seen from any of the

fluctuation measures for WDT. One traditionally used measure in this regard is the relative behavior of the tail of nearest-neighbor spacing distribution $P(s, \Lambda)$, defined as $\alpha(\delta, \Lambda) = \int_0^\delta (P(s, \Lambda) - P_w(s))ds / \int_0^\delta (P_p(s) - P_w(s))ds$ with δ as any one of the crossing points of $P_w(s)$ and $P_p(s)$ (here subscript w and p refer to the Wigner-Dyson case and Poisson case respectively) [9]. In the limit $N \rightarrow \infty$, $\alpha = 0$ and 1 for Wigner-Dyson and Poisson limit respectively. The figure 1 shows the numerically obtained behavior of α (for $\delta \approx 2.02$) with respect to $|z - c| (=|\mu - \mu_c|N^{-2})$ for a fixed c (arbitrarily chosen) with z as a variable; Here z and c are the values of the parameter μN^{-2} for a general BE and a critical BE respectively. The constant value of α at $|z - c| = 0$ for different N -values confirms the size-independence of the level-statistics of BE with parameter $\mu = cN^2$ and therefore its critical nature; it can similarly be verified for other c -values (see figures (6,7) also). Further the convergence of α -values for BEs with different μ and N -values on two branches indicates the presence of a scaling behaviour in the level-statistics of BEs with $|z - c| (=|\mu - \mu_c|N^{-2})$ as the scaling parameter.

III. ANALOGY BETWEEN BROWNIAN ENSEMBLES AND ANDERSON ENSEMBLES

The same evolution equations of P for AE and BE imply a similarity in their eigenvalue distributions for all Y -values, under similar initial conditions (that is, $P(\mu, Y_0)$ same for both the cases). As a result, one obtains the analogous evolution equations for their correlations R_n too. The level density $R_1(E, Y - Y_0)$ of an AE is therefore given by the level-density of the BE with same $|Y - Y_0|$ value (and appearing in a Poisson to Wigner-Dyson transition). Similarly, the analogy of evolutions of R_n ($n > 1$) in the two cases implies (i) the discontinuity of their transition for infinite size of Anderson matrix, (ii) a smooth crossover of R_n for finite system sizes, (iii) the parameter governing the smooth crossover of R_n for finite AEs is given by eq.(14) with $Y - Y_0$ given by eq.(4) and Δ_η as the local mean level spacing for AE (see [10] also). The implication (i) and (ii) are well in agreement with known results about AE-correlations [11]. The implication (iii) indicates the single parametric dependence of the level statistics for AEs. The R_n of an AE are therefore given by those for a BE with a same Λ value although their Y -parameters (as well as level densities) may be different; the Λ -value for the AE and BE will henceforth be referred as Λ_a and Λ_b , respectively. The level-statistics at each Λ_a value of a finite-size AE is then given by a BE with its parameter μ satisfying the condition $\Lambda_a = \Lambda_b$ where $\Lambda_b = R_1^2/4\gamma\mu$ with R_1 as the level-density of the BE; the determination of Λ_a is explained later by using an example. As the BEs with different combinations of the parameters μ and N can have same value of Λ_b ,

the correlations of a given AE can be modeled by many BEs. However the critical BE corresponding to a critical AE is unique; this can be understood as follows. Using $\Lambda_a = \Lambda_b = (4\pi\gamma c)^{-1}e^{-E^2}$, the parameter c for a critical BE corresponding to an AE can be given by

$$c = (4\pi\gamma\Lambda_a)^{-1}e^{-E^2} \quad (15)$$

As shown below by an example, the Λ_a for an AE, away from its critical point, is size-dependent and therefore corresponds to different c values (that is, different critical BEs) for different system sizes. However, Λ_a for a critical AE being size-independent, its critical BE model remains same for all system sizes.

Let us consider the example G given in section 2; its Y parameter is given by eq.(5). The initial state G_0 has the parameter Y_0 same as that of the initial state chosen in the BE case in Section II. Note as $N|Y - Y_0| \rightarrow$ an N -independent constant, the R_1 for the ensemble G is given by eq.(13) which gives $\Delta = (NF)^{-1}$. The parameter Λ for the AE is thus given by eq.(14):

$$\Lambda_a(E, Y) = \left(\frac{|\alpha - \alpha_0|F^2}{\beta\gamma} \right) \eta^2 N^{-(1+\epsilon)} \quad (16)$$

with $F(E)$ giving the energy-dependence of the Λ . Here the correlation volume η , can be obtained by a knowledge of the inverse participation ratio I_2 . As well-known, I_2 shows, at the critical point, an anomalous scaling with the system size L [12]: $I_2 \propto L^{-D_2}$ with D_2 as the multifractality exponent. This gives $\eta = \eta_0 N^{D_2/d}$ with η_0 as a size-independent constant and a function of disorder only. Thus for finite systems

$$\Lambda_a = \left(\frac{|\alpha - \alpha_0|\eta_0 F^2}{\beta\gamma} \right) N^{(2D_2/d)-\epsilon-1} \quad (17)$$

The smooth increase of Λ_a with varying $|\alpha - \alpha_0|$ as a result induces a crossover of the level-statistics from Poisson \rightarrow Wigner-Dyson ensemble. The intermediate level-statistics at each Λ value of a finite-size AE is then given by a $N_1 \times N_1$ BE with its parameter μ given as follows,

$$\mu \approx (4\pi|\alpha - \alpha_0|\eta_0 F^2)^{-1} \beta N^{1+\epsilon-(2D_2/d)} R_1^2 \quad (18)$$

with $R_1 \equiv R_1(E; \mu, N_1)$ as the level-density of the BE. As obvious, the determination of μ from the above equation is not easy, its both sides being μ -dependent. The R_1 for the critical BEs being μ -independent (given by eq.(11)), it is therefore preferable to choose them as model; the substitution of eq.(17) in eq.(15) gives the c -parameter for the corresponding critical BE:

$$c \approx (4\pi|\alpha - \alpha_0|\eta_0 F^2 e^{E^2})^{-1} \beta N^{1+\epsilon-(2D_2/d)} \quad (19)$$

Thus each state of disorder in an AE of size L ($N = L^d$) can be modeled by a critical BE with the parameter c

given by eq.(19). Note, c being energy-dependent, different energy ranges of a given AE will, in general, correspond to different critical BEs.

For disordered systems with infinite system size ($L \rightarrow \infty$), the strong dimensional sensitivity of η and thereby Λ gives rise to dimensional dependence of the level statistics. For example, for an infinitely long one dimensional lattice with z nearest neighbors, the statistics is known to remain Poisson irrespective of the disorder strength. In terms of Λ , this behavior can be explained as follows: here $\eta \approx z^2$ [13] giving $\Lambda_a \simeq o(z^2/L) \rightarrow 0$ for $N = L \rightarrow \infty$ unless there is a very long range connectivity in the lattice (i.e $z \approx \sqrt{L}$). However, according to AE-BE analogy, a crossover from Poisson to Wigner-Dyson ensemble can be seen for finite L by varying the ratio z^2/L or, equivalently, Λ_a ; this in agreement with earlier studies [13].

For infinite systems with dimension $d > 2$, the change of disorder (or energy) leads to a discontinuous change in the correlation volume η and thereby Λ . Earlier numerical studies have suggested that the level statistics, at the critical point, is size independent and belongs to a universality class different from that of metal or insulator regime. The existence of such a statistical behavior requires Λ_a to be size-independent at the critical point (i.e. N -independence of Λ_a in eq.(17)). This in turn suggests that $D_2 = d(1 + \epsilon)/2$ at the critical point ($\epsilon(z) \ll 1$). Note the critical point D_2 -value obtained by various numerical experiments on a three dimensional AE system fluctuates in the range 1.4-1.6 [17,20,24,25]. The value $D_2 = 1.5(1 + \epsilon)$ suggested by our formulation for the case $d = 3$ is, therefore, in good agreement with earlier studies. (The observed fluctuations of numerically obtained D_2 about the value 1.5 seem to be the effect of its calculation in the critical regime rather than at exact critical point; it may also be due to numerical accuracy). Using the above prediction for D_2 , the c parameter of the critical BE analog (for correlations), for the critical state of the AE example G can be given as follows:

$$c \approx (4\pi|\alpha - \alpha_0|\eta_0 F^2 e^{E^2})^{-1} \beta \quad (20)$$

In general, the definition of Λ can be used to determine the existence of a critical point level statistics in the systems modeled by Gaussian ensembles. For example, for a disordered system, with $|Y - Y_0| \simeq o(N^{x_1})$, $R_1 \simeq o(N^{x_2})$ and $\eta \propto N^{D_2/d}$, a critical point of its level-statistics can exist only if the wavefunction dynamics gives rise to an exponent $D_2 \approx d(2 - x_1 - 2x_2)/2$. The critical point of the level statistics is therefore very sensitive to the wavefunction dynamics. (Note, as $x_1 = -2$, $x_2 = 1$ for a BE, the existence of its critical point requires $D_2 = d$. For a critical BE, therefore, $\eta \propto N$ which however is indeed the case as shown by the eigenfunction studies of BEs).

The information about dimensionality of the system enters in Λ_a through η as well as $|Y - Y_0|$. The AEs with different dimensionality can have different critical values

of Λ_a and, therefore, correspond to critical BE analogs with different c values. A knowledge of Λ_a can then be used to map the critical level statistics at MIT for various dimensions $d > 2 \rightarrow \infty$ to the infinite family of critical BEs.

In general, Λ_a is a function of coordination number, disorder strength, hopping rate and dimensionality of the lattice as well as the level-density of the system. Further the boundary conditions/ topologies, leading to different sparcity and coordination numbers, can also result in different critical level statistics even if the underlying symmetry and the dimensionality is same; this is in agreement with numerical observations [17] and analytical study for 2D systems [18].

IV. DETERMINATION OF FLUCTUATION MEASURES FOR MIT

Many results for the spectral fluctuations of the WDT with Poisson ensemble as an initial state are already known [7] and can directly be used for the corresponding measures for the MIT in different disordered systems.

A. MIT With No Time-Reversal Symmetry

The fluctuation measures, for the Anderson transition in presence of a magnetic field, can be given by the BEs appearing during a WDT which violates time-reversal symmetry. Such a WDT, occurring in a complex Hermitian matrix space (that is $\beta = 2$), corresponds to a transition from Poisson \rightarrow GUE ensembles.

(i) The 2-Level Density Correlator $R_2(r; \Lambda)$:

The R_2 for BEs during Poisson \rightarrow GUE transition has been obtained by various studies [15,7,19]. Here we use the form given in [15] for the purposes to be explained later (note, our Λ is equivalent to $\Lambda^2/2$ used in the [15]),

$$R_2(r; \Lambda) = 1 + \frac{4\Lambda}{r} \int_0^\infty du F e^{-2\Lambda u^2 - 4\pi\Lambda u} \quad (21)$$

with

$$\begin{aligned} F &= \sin(ur)f_1 - \cos(ur)f_2 \\ f_1 &= (2/z)[I_1(z) - \sqrt{8u/\pi}I_2(z)] \\ f_2 &= (1/u)[I_2(z) - \sqrt{2u/\pi}I_3(z)] \end{aligned} \quad (22)$$

where $z = \sqrt{32\pi\Lambda^2u^3}$ and I_n as the n^{th} Bessel function. (Note, the eq.(4.15) in [15] has a misprint in the coefficient of u is the exponent; the correct coefficient is given in our eq.(21)).

The eq.(21) gives the exact form of two-point correlation for the Anderson transition with no time-reversal

symmetry. Here $R_2(r, \infty) = 1 - (\sin^2(\pi r)/\pi^2 r^2)$ and $R_2(r, 0) = 1$ corresponding to metal and insulator regime respectively. A substitution of critical value of Λ_a in eq.(21) will thus give R_2 for the critical AE.

For large Λ -values (for all r), R_2 can be approximated as follows [15,19]: $R_2 = 1 - Y_2$ where

$$\begin{aligned} Y_2(r, \Lambda) &= \frac{-4\Lambda}{16\pi^2\Lambda^2 + r^2} - \frac{1}{2\pi^2 r^2} [\cos(2\pi r)e^{-\frac{r^2}{2\Lambda}} - 1] \quad (23) \\ &\approx \frac{3}{2\pi^2\Lambda} \frac{\sin^2(\pi r)}{\sinh^2(r\sqrt{3/2\Lambda})} \quad (\text{for } r \ll \sqrt{\Lambda}) \end{aligned}$$

However, for $r > \sqrt{\Lambda}$, $Y_2(r, \Lambda) = -\frac{4\Lambda}{16\pi^2\Lambda^2 + r^2} + \frac{1}{2\pi^2 r^2}$. As $\Lambda_b = (4c\pi\gamma)^{-1}$ (near $E = 0$) for a critical BE, the $Y_2 \approx (1 - 8\pi^2\Lambda_b)/2\pi^2 r^2$ for $r > 2\beta\pi\Lambda_b$ (here $\beta = 2$).

The above large r -behavior of $Y_2(r; \Lambda)$ at $\Lambda = \Lambda_b$ results in a non-zero, fractional value of the sum $I = \int_{-\infty}^{\infty} Y_2(r; \Lambda) dr$ for a critical BE of complex-Hermitian type:

$$I \approx 1 - (\beta\pi^2\Lambda_b)^{-1}. \quad (24)$$

Note a $0 < I < 1$ value is believed to be an indicator of the multifractality of the wavefunctions and the fractional compressibility of the spectrum; (I is one and zero for the WD and Poisson case, respectively) [20,21]. A fractional behavior of I and the multifractality is already known to exist in critical AE [20,21]. Using $\Lambda_a = \Lambda_b$ in eq.(24), one can now determine the measure I for an AE: $I \approx 1 - (\beta\pi^2\Lambda_a)^{-1}$.

(ii) Nearest Neighbor Spacing Distribution $P(S)$

The nearest-neighbor spacing distribution $P(s)$ for the MIT with no time-reversal symmetry can similarly be given by using the one for the BE during Poisson \rightarrow GUE transition [22,32]:

$$P(s; \Lambda) \propto \frac{s}{\sqrt{2\pi\Lambda}} e^{-s^2/8\Lambda} \int_0^\infty dx e^{-x-x^2/8\Lambda} \frac{\sinh(xs/4\Lambda)}{x}. \quad (25)$$

(Although this result is rigorous for 2×2 matrix space but is proved reliable for systems with many levels; see [32]). Note $P(s; \infty) = P_w(s) = 32s^2 e^{-4s^2/\pi}/\pi^2$ (WD limit) and $P(s; 0) = P_p(s) \propto e^{-s}$ (Poisson limit), thus giving the correct asymptotic behavior.

(iii) Level-Compressibility

The level compressibility $\chi = 1 - \int_{-\infty}^{\infty} Y_2(r) dr = 1 - I$ is an important characteristic of the critical level statistics and the multifractal nature of the wavefunctions.

The χ for a BE can be obtained by using eq.(21),

$$\chi(\Lambda) = 1 - 4\pi\Lambda \int_0^\infty du f_1(z) \exp[-2\Lambda u^2 - 4\pi\Lambda u] \quad (26)$$

$$\approx (\beta\pi^2\Lambda)^{-1} \quad \text{for large } \Lambda \quad (27)$$

Thus a critical BE characterized by a finite c value ($< \pi/4$) shows a fractional level-compressibility: $\chi \approx 4\gamma c/\beta\pi$; As can be seen from eq.(26), $\chi \rightarrow 1$ for $\Lambda \rightarrow 0$ corresponding to a Poisson ensemble and $\chi \rightarrow 0$ for $c \rightarrow 0$ or $\Lambda \rightarrow \infty$ which corresponds to the GUE.

The numerical studies on some AE systems indicate that the χ takes a fractional value at the hybrid phase near the critical point; it is zero and one in the metallic and the insulator phase, respectively. The existence of a fractional χ for both critical BE and critical AE is consistent with our claim of their spectral analogy. The compressibility of the AE with different types of disorders and lattices can now be obtained just by finding the same for their critical BE analogs.

B. MIT With Time-Reversal Symmetry

The statistical measures for the Anderson transition in presence of a time-reversal symmetry can similarly be obtained by using their equivalence to a WDT preserving the same symmetry, that is, a transition from Poisson \rightarrow GOE ensembles; the later occurs in a real-symmetric matrix space (here $\beta = 1$). However due to the technical difficulties [7]), only some approximate results are known for the latter case.

(i) The 2-Level Density Correlator $R_2(r; \Lambda)$:

The R_2 for small- r can be obtained by solving eq.(17) of [2] for $\beta = 1$ which gives

$$R_2(r, \Lambda) \approx (\pi/8\Lambda)^{1/2} r e^{-r^2/16\Lambda} I_0(r^2/16\Lambda) \quad (28)$$

with I_0 as the Bessel function.

Similarly for large- r behavior, R_2 can be shown to satisfy the relation (see eq.(21) of [7])

$$R_2(r, \Lambda) \approx R_2(r, \infty) + 2\beta\Lambda \int_{-\infty}^{\infty} ds \frac{R_2(r-s; 0) - R_2(r-s; \infty)}{(s^2 + 4\pi^2\beta^2\Lambda^2)} \quad (29)$$

$$\approx R_2(r, \infty) + 2\beta\Lambda/(r^2 + 4\pi^2\beta^2\Lambda^2) \quad (30)$$

where $\beta = 1$ and $R_2(r, \infty) = 1 - \sin^2(\pi r)/\pi^2 r^2 - (\int_r^{\infty} dx \sin \pi x / \pi x) (\frac{d}{dr} \sin \pi r / \pi r)$ (GOE limit).

As can be seen from the above, $Y_2(r, \Lambda) \approx -\frac{2\Lambda}{4\pi^2\Lambda^2 + r^2} + \frac{1}{2\pi^2 r^2}$ for $r > \sqrt{\Lambda}$. However, note, for $r > 2\pi\Lambda$, the behavior of Y_2 is different from that of a BE with no TRS: $Y_2 \approx (1 - 4\beta\pi^2\Lambda)/2\pi^2 r^2$. This further suggest following behavior of I : $I = 1 - (\beta\pi^2\Lambda)^{-1}$. The I for a critical BE is therefore symmetry-dependent; (as $\Lambda = \Lambda_b$ does not depend on β). However the I for its AE analog is independent of the symmetry parameter β ; this is because $\Lambda = \Lambda_a \propto \beta^{-1}$ in this case (see eq.(17)).

(ii) Nearest Neighbor Spacing Distribution $P(S)$

The $P(s)$ for this case can be given by using the one for a BE during Poisson \rightarrow GOE transition [22]:

$$P(s, \Lambda) = (\pi/8\Lambda)^{1/2} s e^{-s^2/16\Lambda} I_0(s^2/16\Lambda) \quad (31)$$

with I_0 as the Bessel function; note, as expected, this is same as R_2 behavior for small- r (eq.(28)).

(iii) Level-Compressibility

The lack of the knowledge of $R_2(r, \Lambda)$ for entire energy-range handicaps us in providing an exact form of the compressibility for the time-reversal case. However its approximate behavior can be obtained by using the relation $\chi = 1 - I$. Thus, for a time-reversal critical BE ($\beta = 1$) with finite c value ($\Lambda_b = (4\gamma c\pi)^{-1}$),

$$\chi \approx (\beta\pi^2\Lambda_b)^{-1} \quad (32)$$

and therefore $\chi \approx (\beta\pi^2\Lambda_a)^{-1}$ for its AE analog. The eq.(32) indicates the influence of the underlying symmetry on the compressibility of the levels of a critical BE. However as $\Lambda_a \propto \beta^{-1}$ (see eq.(17)), the χ for a critical AE would be symmetry-independent; this is in agreement with numerical observations for Anderson systems [9,25]. This further implies that the critical BEs corresponding to critical AEs with and without time-reversal symmetry would be different.

V. NUMERICAL COMPARISON OF THE LEVEL-STATISTICS OF CRITICAL AE AND CRITICAL BE

In this section, we investigate the AE-BE spectral analogy by numerically comparing some of their fluctuation measures, namely, $P(s)$ and the number variance $\Sigma^2(r) = \langle (r - \langle r \rangle)^2 \rangle$. The former is a measure of the short-range correlations in the spectrum and the latter, describing the variance in the number of levels in an interval of r mean level spacings, contains the information about the long-range correlations [3]. The Σ_2 is also an indicator of the compressibility of the spectrum; $\lim r \rightarrow \infty \Sigma_2(r) \approx \chi r$.

We study each AE case for two system sizes by considering two ensembles of 1200 and 400 matrices for sizes $L = 10$ and $L = 13$, respectively. Each BE (chosen with $\gamma = 2$) is also analyzed for two dimensions $N = 1000$ and 3000, consisting of 1600 and 600 matrices respectively. The reason for the choice of a larger ensemble for the BE case is following. As the transition of the fluctuation measures is governed by Λ , an energy dependent variable, the rate of transition is different in different parts of the spectrum for both AE and BE. To avoid mixing of the levels with different transition rates, we used only 100 unfolded levels from middle of the spectrum (near $E=0$)

of each Anderson matrix (which gives a total of approximately 10^5 and 40000 levels for sizes $L = 10$ and $L = 13$, respectively). However, as shown below, the decay of R_1 is rapid for each BE case; as a result, only 55 – 60 unfolded levels were taken from the spectrum near $E = 0$ for each BE matrix; a bigger ensemble was therefore required to keep the total number of levels nearly same as in AE case. (The unfolding of each spectrum was carried out by numerically calculating the unfolded levels $r_j = \int_{-\infty}^{E_j} dx R_1(x)$ for $(j = 1, 2, \dots, N)$ with symbol E_j used for levels before unfolding).

To study the analogy in presence of different physical conditions e.g. symmetry, boundary conditions, random and non-random hopping, we consider five cases of the 3-dimensional AE (simple cubic lattice of size $L = 13$) with Gaussian site disorder in the critical regime (the information about the exact critical points for the Gaussian disorders is not available):

(i) **AE₁** : The AE with isotropic non-random hopping, periodic boundary conditions and time-reversal symmetry ($\beta = 1$); here $W = 21.3$, $W_1 = 0$, $W_2 = 0$, $t_1 = 1$, $t_2 = 0$. The existence of the criticality at these values of the disorder parameters is numerically verified in [23].

(ii) **AE₂** : The AE with isotropic random hopping, hard wall boundary conditions and time-reversal symmetry; here $W = 4.05$, $W_1 = 1$, $W_2 = 0$, $t_1 = 0$, $t_2 = 0$. The criticality of AE for same disorder parameter values but with periodic boundary conditions is numerically studied in [26]. However the system remains in the critical regime under hard wall boundary conditions too.

(iii) **AE₃** : Same as AE₁ but with $W = 30$. The purpose for considering the same Anderson system at two different disorder values is to show that the statistics near the critical point of a finite system undergoes a smooth variation (thus indicating the presence of a critical regime).

(iv) **AE₄** : The AE with isotropic non-random hopping, periodic boundary conditions and no time-reversal symmetry; here $W = 52.2$, $W_1 = 0$, $W_2 = 0$, $t_1 = 1$, $t_2 = 1$. Here the time-reversal symmetry is broken by implying an Aharnov Bohm flux ϕ which gives rise to a nearest neighbor hopping $H_{kl} = \exp(i\phi)$ for all k, l values related to the nearest-neighbor pairs [25]. Here the flux ϕ is chosen to be non-random in nature, that is, $\langle \cos^2(\phi) \rangle = W_1 = 0$, $\langle \sin^2(\phi) \rangle = W_2 = 0$ and $\langle \cos(\phi) \rangle = t_1 = 1$, $\langle \sin(\phi) \rangle = t_2 = 1$.

(v) **AE₅** : The AE with isotropic random hopping, hard wall boundary conditions and no time-reversal symmetry; here $W = 9.92$, $W_1 = 1$, $W_2 = 1$, $t_1 = 0$, $t_2 = 0$. Here again an Aharnov Bohm flux ϕ is used to break the time-reversal symmetry which gives $H_{kl;1} = \cos(\phi)$ and $H_{kl;2} = \sin(\phi)$ for all nearest neighbor interactions. As obvious, a random variation of ϕ is required to get the random hopping in the lattice.

Here the cases AE₁, AE₂, AE₃, and, therefore their BE

models, are ensembles of real-symmetric matrices (due to presence of time-reversal symmetry). Similarly AE₄, AE₅ and corresponding BEs are ensembles of complex hermitian matrices due to absence of time-reversal symmetry.

The parameter $Y - Y_0$ in each AE case has been obtained by using eq.(5) which gives $N|Y - Y_0| \simeq o(1)$. The BE-AE analogy suggests, therefore, that the mean level-density R_1 for all five AE cases should be given by eq.(13); $R_1 = NF$ with F as an N -independent function of energy. This is confirmed by our numerical analysis of R_1 for different N -values, with Fig.2(a) showing the comparison only for two N -values, for each AE case. (Note, for R_1 study, the spectrum is not unfolded and almost all eigenvalues of each matrix are used for the analysis). The $\alpha - \alpha_0$ value calculated from eq.(6) and the numerically fitted function $F = \sqrt{\pi}f_1 e^{-x^*x/f_2}$ for each AE case is given in Table I. Using the values in eq.(17), one can obtain Λ_a for each case. However the determination of the c parameters of their critical BE analogs would require a prior knowledge of the η_0 and D_2 . The lack of such an information compels us to obtain the c parameter by a numerical search of the critical BE analog for the $P(s)$ and Σ^2 measures of each AE case. As already mentioned, the Λ being the transition parameter for higher order correlations, the so obtained critical BE analog need not have a same mean level density R_1 . The behavior of R_1 for the critical BE analogs of the correlations for the five AE cases is shown in figure 2(b); the numerical fitting confirms that $R_1 = (N/\sqrt{\pi})e^{-E^2}$ for each critical BE case which is quite different from their AE analogs.

The figures 3,4,5 show the numerically studied behavior of the measures $P(S)$ and $\Sigma_2(r)/r$ for the cases (i-v). The almost same behavior for two system sizes in each case for both the measures indicates the considered disorder parameters being close to their critical values. As shown in the figures, a critical BE analog with approximately similar behavior of these measures exist for each AE case; see Table II for the c values of their BE analogs. Note, the measures $P(S)$ and Σ_2 for various critical BEs are size-independent, as expected from the N -independence of Λ_b ; this is also confirmed by their behavior shown in figures 6,7. Further, as shown in Table II for $r = 20$, the χ values suggested by the large- r behavior of $\Sigma^2(r)/r$, are quite close to those given by the eqs.(27,32), namely, $\chi \approx 4\gamma c/\beta\pi$.

In past, various studies [4,33] of critical level statistics of AE indicate that, for large level spacings, the measure $P(s)$ behaves as $P(s) \sim \exp(-\kappa s)$. It has also been claimed that κ is related to the compressibility: $\kappa \approx (1/2)\chi$; the χ being symmetry-independent for a critical AE, κ is also symmetry independent. Our numerical study indicates a similar tail behaviour of $P(s)$ for critical BE too. The figure 8 shows the comparison of nu-

merically obtained level-spacing distribution for some of the critical BEs with function $e^{-\kappa s}$; we find $\kappa \approx \beta\pi/8\gamma c$ for these cases. Thus χ - κ relation for a BE is similar to that of an AE: $\kappa = (1/2)\chi$.

To check that the numerically analogous critical BEs of the five AE cases are same as those predicted by our analytical study, namely, eq.(19), a prior knowledge of correlation length η and therefore statistical analysis of wavefunctions is required; we hope to verify it in near future. As the purpose of our numerical study was just to provide additional support to our exact analytical results by showing the existence of a critical BE corresponding to each AE case, we have confined ourselves to finding only the closely agreeing values of the parameters for the BE analogs and have not calculated any error bars.

The study [21] claims that the critical level-statistics in the Rosenzweig-Porter ensemble (same as BE, as mentioned in section II) does not have a fractional compressibility and, therefore, is different in nature from the one for critical AE. However our analytical results supported by the numerical evidence, presented in this paper, disprove the above claim. The existence of a non-fractional χ increasing with c for various critical BEs can be seen from the figures 6,7; the numerically obtained χ is close in agreement with our analytical prediction, namely, eq.(32). Note, the presence of a fractional compressibility in an ensemble essentially same as critical BE, and, its possibility as a model for critical AE was also suggested in [14] which was later on contradicted in [16]. Our work suggests that the existence of the fractional compressibility in a sequence of levels depends on the competition between the complexity parameter $|Y - Y_0|$ and the local level density.

VI. CONNECTION WITH PRBM MODEL

In past, a random matrix ensemble, namely, power law random banded matrix (PRBM) ensemble was suggested as a possible model for the critical level statistics of Anderson Hamiltonian [30]. A PRBM ensemble is defined as the ensemble of random Hermitian matrices with matrix elements H_{ij} as independently distributed Gaussian variables with zero mean i.e $\langle H_{ij} \rangle = 0$ and the variance $\langle H_{ij}^2 \rangle = a^2(|i - j|)$ where $a^2(r) = [1 + (r/b)^2]^{-1}$. It is critical at arbitrary values of the parameter b and is believed to show all the key features of the Anderson critical point, including multifractality of eigenfunctions and the fractional spectral compressibility.

The PRBM-AE connection is a special case of our study connecting any generalized Gaussian ensemble (GGE) with AE. The PRBM ensemble being Gaussian in nature, its complexity parameter can be defined by using eq.(4) which can then be used to obtain its BE analog.

The eq.(4) gives $Y - Y_0 \propto b/N$ (for $b \gg 1$) which leads to the parameter Λ for a PRBM ensemble: $\Lambda \propto b$. The spectral compressibility χ for a PRBM ensemble can now be obtained by using PRBM-BE analogy which gives, by using eq.(32), $\chi \propto b^{-1}$ for large b which is in agreement with [30].

Note, the parameter $Y - Y_0 \approx o(1/N)$ for both AE and PRBM which results in similar N -dependence for R_1 and thereby rate of change of Λ with respect to energy in the two cases. Thus PRBM is a better model for numerical comparison with AE especially if the transition is occurring due to the change of energy.

In brief, the studies suggesting the analogy of spectral statistics for the PRBM and AE ensembles are well in agreement with our study claiming the AE-BE analogy.

VII. CONCLUSION

In the end, we re-emphasize our main results:

(i) Under independent electron approximation, the level-statistics for the disordered systems undergoing localization \rightarrow delocalization transition of wavefunctions can be described by the Brownian ensembles (with uncorrelated elements) undergoing a similar transition.

(ii) The level-statistics in the disordered systems without electron-electron interaction is shown, analytically, to be governed by a single scaling parameter $\Lambda = \frac{|Y - Y_0|}{\Delta^2} \frac{\eta^2}{N^2} = f(\frac{\eta}{N})$. The second equality follows from the dependence of wavefunction statistics e.g inverse participation ratio I_2 and therefore η on the complexity parameter $|Y - Y_0|$.

(iii) The level-statistics is therefore governed by the competition between complexity parameter and local mean level spacing. The critical point of level statistics occurs when the complexity parameter $Y - Y_0$ and Δ_η have same size dependence. In particular, if $|Y - Y_0| \sim o(N^\alpha)$ and $\Delta_\eta \sim o(N^\beta)$ for an AE, its critical point will occur when $\alpha - 2\beta = 0$. However if the local mean level spacing in the system changes at a faster rate with size as compared to $\sqrt{Y - Y_0}$ (i.e $\beta > \alpha/2$), the system will never reach its critical state and will always remain in the localized regime.

(iv) The critical BE model corresponding to a critical AE is unique. Further, it is different for critical AE with and without time-reversal symmetry.

(v) The AE-BE analogy suggest the symmetry-independence of the compressibility of levels and the multifractality of the wavefunctions at the critical point of Anderson transition. Further the multifractality exponent D_2 is predicted to be given by $D_2 = d(1 + \epsilon)/2$ for a d -dimensional Anderson system.

(vi) Similar to AEs, the level-statistics of BEs shows a scaling behavior as well as a critical point with fractional level-compressibility. However, unlike AEs, the χ turns

out to be symmetry dependent for BEs, their parameter Λ being symmetry independent.

It should be noted that both MIT as well as WDT occur due to delocalization of the wavefunctions. In fact, our analytical study suggests that the level-statistics of all complex systems undergoing a localization \rightarrow delocalization transition follows the same route although with different transition rates; the state of level-statistics of two systems with different complexity may correspond to two different points on this route. In principle, our analytical work is applicable to the Gaussian models of complex systems only, however the intuition based on earlier studies suggest the validity of the results for the systems with other origins of randomness too [3]. For example, the investigation of a number of dynamical systems seems to support this intuition. It has been shown that the spectral statistics of pseudo-integrable billiards is remarkably similar to the critical statistics of AE [27]. The presence of a statistics intermediate between the Poisson and GOE has already been shown for the Kicked rotor in the non-integrable regime of the kicking parameter [31]. A correspondence of the integrable systems to the insulators and of the chaotic systems to the metals is already known to exist. The Integrability \rightarrow chaos transition in the dynamical systems therefore seems to follow a route in the level-statistics similar to that of MIT; note such a transition in classical systems corresponds to a delocalization of the wavefunctions in their quantum analog. The analogy of the statistical level fluctuations between AE and BE can thus be extended to dynamical systems and BE too; the latter information can then be used to obtain the correlations for the non-integrable regime.

The evidence of such an analogy would suggest the existence of several features, unknown so far, for the level statistics of dynamical systems. For example, the analogy can be used to intuitively claim and search for the existence of a critical point, the dimensional dependence of level-statistics and the multifractality of eigenfunctions during the transition from Integrable to chaotic dynamics. Such a critical point of level-statistics may correspond to the classical regime near the breaking of last KAM Curve. It should be noted that a generic one-dimensional dynamical system always shows a Poisson level-statistics (in analogy with one-dimensional AE). However the dynamics in a 3-dimensional system shows a feature namely "Arnold Diffusion", absent in lower dimensions. The intuition based on the above analogy suggests the possible existence of a critical level statistics at the parametric values at which Arnold Diffusion takes place. A further exploration of such an analogy is therefore highly desirable.

- [1] F.Dyson, *J. Math. Phys.* 3, 1191 (1962).
- [2] P.Shukla, *Phys. Rev. E* 62, 2098, (2000);
- [3] M.L.Mehta, *Random Matrices*, Academic Press, (1991).
- [4] B.I.Shklovskii, B.Shapiro, B.R.Sears, P.Lambrianides and H.B.Shore, *Phys. Rev. B*, 47, 11487 (1993).
- [5] A.G.Aronov and A.D.Mirlin, *Phys. Rev. B*, 51, 6131, (1995).
- [6] F.Haake, **Quantum Signature of Chaos**, Springer, Berlin (1991).
- [7] A.Pandey, *Chaos, Solitons and Fractals*, 5, (1995).
- [8] B.Shapiro, *Int.J.Mod.Phys. B*, 10, 3539, (1996).
- [9] E.Hofstetter and M.Schreiber, *Phys. Rev. B*, 49, 14726, (1994).
- [10] The higher order correlations basically being the measures of the fluctuations of the density around its average value, their comparison in two different spectrum makes sense only if the fluctuations are measured with respect to same background. This requires an unfolding of each spectrum, that is, rescaling by its mean level density before comparison with another spectrum [3,6]. As the parameter governing the evolution in the rescaled spectrum is Λ , the higher order correlations of an AE are given by a BE with a same Λ value.
- [11] A.G.Aronov, V.E.Kravtsov and I.V.Lerner, *Phys. Rev. Lett.*, 74, 1174, (1995).
- [12] F.Wegner, *Z.Phys.B* 36, 209, (1980).
- [13] Y.V.Fyodorov and A.D.Mirlin, *Int.Jou.of Mod.Phys.B*, 8, 3795, (1994).
- [14] M.F.Hussein and M.P.Pato, *Phys. Rev. Lett.* 80, 1003, (1998).
- [15] H.Kunz and B.Shapiro, *Phys. Rev. E*, 58, 400, (1998).
- [16] M.Janssen, B.Shapiro, I.Varga, *Phys. Rev. Lett.* 81, 3048, (1998).
- [17] D.Braun, G.Montambaux and M.Pascaud, *Phys. Rev. Lett.* 81, 1062, 1998.
- [18] V.E.Kravtsov and V.I.Yudson, *Phys.Rev.Lett.* 82, 157, 1999.
- [19] K.M.Frahm, T.Guhr, A.Muller-Groeling, *Ann. Phys. (N.Y.)* 270, 292 (1998).
- [20] J.T.Chalker, V.E.Kravtsov and I.V.Lerner, *Pis'ma Zh. Eksp. Teor. Fiz.* 64, 355 (1996) [*JETP Lett.* 64, 386, (1996)].
- [21] V.E.Kravtsov and K.A.Muttalib, *Phys.Rev.Lett.* 79, 1913, (1999).
- [22] S.Tomsovic, Ph.D Thesis, University of Rochester (1986); V.K.B.Kota and S.Sumedha, *Phys. Rev. E*, 60, 3405, (1999).
- [23] K.Slevin and T.Ohtsuki, *Phys. Rev. B*, 63, 045108, (2001);
- [24] T.Brandes, B.Huckestein and L.Schweitzer, *Ann.Phys. (Leipzig)*, 5, 633, (1996); T.Ohtsuki and T.Kawarabayashi, *J.Phys.Soc.Japan*, 66, 314 (1996); I.Kh.Zharekeshev and B.Kramer, *Jpn. J. Appl. Phys.* 34, 4361, (1995); M.L.Ndawana, R.A.Romer and M.Schreiber, *Eur. Phys. J.B* 27, 399-407 (2002).
- [25] T.Terao, *Phys.Rev.B*, 56, 975, (1997).
- [26] P.Biswas, P.Cain, R.A.Romer and M.Schreiber, *cond-mat/0001315*;
- [27] E.Bogomolny, U.Gerland and C.Schmit, *Phys. Rev. E* 59, R1315 (1999).

- [28] K.A.Muttalib, Y.Chen, M.E.H.Ismail and V.N.Nicopoulos, Phys. Rev. Lett. 71, 471 (1993).
- [29] M.Moshe, H.Neuberger and B.Shapiro, Phys. Rev. Lett. 73, 1497 (1994).
- [30] A.D.Mirlin et.al., Phys.Rev.E, 54, 3221, (1996); F.Evers and A.D.Mirlin, cond-mat/0001086, cond-mat/0003332; I.Verga and D.Braun, Phys. Rev. B61 RC11859 (2000).
- [31] T.Dittrich and U.Smilansky, Nonlinearity, 4, 85, (1991).
- [32] G.Lenz and F.haake, Phys. Rev. Lett. 67, 1, (1991).
- [33] L. Schweitzer and H. Potempa, Physica A 266, (1999) 486; H. Potempa and L. Schweitzer, J. Phys.: Cond. Matt. 10 (1998) L431; I. Kh. Zharekeshev and B. Kramer, Phys. Rev. Lett. 79 (1997) 717; M. Batsch et. al., Phys. Rev. Lett. 77 (1996) 1552; L. Schweitzer and I. Kh. Zharekeshev, J. Phys.: Cond.Matt. 7 (1995) L377.

FIGURE CAPTIONS

Fig. 1. The scaling behaviour of the integrated nearest-neighbor spacing distribution α during WDT: note α values for BEs with different parameters μ and sizes N converge on the same two curves, thus indicating α dependence on a specific combination of μ and N , namely, $z = \mu/N^2$. Further, at $z = c$, α remains unchanged for different N values, thus indicating a critical point of BEs.

Fig. 2. The behavior of level-density $F(E) = N^{-1} \cdot R_1$:

(a) for the five AE cases in their critical regimes for two system sizes $L = 10$ and $L = 13$. The numerical fitted function has the form $F = f_1 e^{-(E^2/f_2)}$ with f_1 and f_2 values given in Table 1,

(b) for the critical BE analogs of the higher-order correlations of the five cases considered in 2.(a). Here F for all the critical BE cases is well-fitted by the function $F(E) = \pi^{-1/2} e^{-E^2}$. Note the lack of analogy between the mean-level densities for the cases given in 2(a) and 2(b) while their highr order correlations (shown in Figures 3,4,5) are approximately same.

Fig. 3. The comparison of distribution $P(S)$ of the nearest-neighbor spacings S for the AE (3-dimensional) and BE cases:

(a) when time-reversal symmetry is preserved : for AE_1 (with periodic boundary conditions and non-random hopping) and AE_2 (with hard wall boundary conditions and random hopping). The nearly similar behavior of $P(S)$ for two system sizes $L = 13$ and $L = 10$ confirms the critical nature of each AE case. The critical BE (real-symmetric) close to each AE case is also shown in the figure ($c = 0.03$ for AE_1 and $c = 0.1 - 0.2$ for AE_2). Note the $P(S)$ -behavior for AE_1 and AE_2 is different although both belong to same symmetery class and dimensionality; this indicates the system-dependence of short-range correlations at the critical point.

(b)when time-reversal symmetry is broken : for

the cases AE_4 (periodic boundary conditions and non-random hopping) and AE_5 (with hard wall boundary conditions and random hopping) along with their critical BE analogs (now complex hermitian matrices, $c = 0.3$ for AE_4 and $c = 0.03$ for AE_5). Here again the boundary conditions sensitivity of the short-range correlations can be seen by the different $P(S)$ -behavior for AE_4 and AE_5 .

Fig. 4. The comparison of the $\Sigma^2(r)/r$ -behavior for the AE and BE cases. (Note here the critical BE analog for each AE case is same as for the $P(S)$ -study):

(a) Time-Reversal case: AE_1 , AE_2 and AE_3 and the corresponding critical BEs. The large- r behavior of Σ^2/r suggest a fractional value of χ (see Table 2). The cases AE_1 and AE_3 are same in all details except for the diagonal disorder, the former being at the critical point while latter is in the critical regime. Note the $\Sigma^2(r)/r$ behavior of AE_3 does not seem very sensitive to the size although it is slightly away from the critical point. Thus long range correlations in the critical regime (and not only at the critical point) seem to be size-independent however same is not true for short range correlations, as indicated by figure 5. Further the different behaviors of AE_1 and AE_2 cases again confirm the system-dependence of the critical point correlations.

(b) No Time-Reversal symmetry: AE_4 and AE_5 and the corresponding critical BEs. Both AE_4 and AE_5 belong to same symmetry class and dimensionality but show different long-range behavior of levels.

Fig. 5. Here the $P(S)$ -behavior for two system sizes of AE_3 case (Periodic Boundary conditions, non-random hopping and slightly away from critical point) is considered. The different behaviour for two sizes indicates the size-sensitivity of short range correlations in critical regime. Note, as expected, the c parameters of the critical BE analogs for two sizes $L = 13$ and $L = 10$ are slightly different ($c \approx 0.2$ for $L = 13$ and $c \approx 0.15$ for $L = 10$).

Fig. 6. The $P(S)$ distribution for various critical BEs (with time-reversal symmetry i.e $\beta = 1$), each considered for two N -values. The size-independence of the distributions confirms the critical state of the BEs.

Fig. 7. The behavior of $\Sigma^2(r)/r$ for various critical BEs, each considered for two N -values. As can be seen, Σ^2/r for large r seems to approach the limit suggested by the relation $\chi = (4\gamma c/\beta\pi)$. This confirms that each critical BE has an N -independent, fractional χ -value which increases with increasing c .

Fig. 8. The comparison of tail of $P(S)$ distribution for some of the critical BEs with function $e^{-\kappa s}$; The critical BEs chosen here are the ones which are found close to critical AEs considered in figure 3(b). The fitted κ -values seem to satisfy the relation $\kappa = 1/2\chi$ with (i)

$\chi = 0.13$ for $c = 0.03, \beta = 1$, (ii) $\chi = 0.38$ for $c = 0.2, \beta = 1$, (iii) $\chi = 0.10$ for $c = 0.03, \beta = 2$ (iv) $\chi = 0.34$ for $c = 0.3, \beta = 2$. Note the χ values given above are close in agreement with those predicted on the basis of relation $\chi = 4\gamma c/\beta\pi$ (see table II).

Table I: The mean-level density behaviour for the five AE cases. Here the parameter $\alpha - \alpha_0$ is obtained by using eq.(6) and the parameters f_1 and f_2 for the mean level density $R_1 = N\sqrt{\pi}f_1 e^{-x^2/f_2}$ are obtained by a numerical fitting (shown in figure 2(a)).

Case	$(\alpha - \alpha_0)$	f_1	f_2
AE_1	3.62	0.036	100
AE_2	1.36	0.161	5
AE_3	4.32	0.024	170
AE_4	5.43	0.016	400
AE_5	2.05	0.058	40.

Table II: The C parameters for the critical BE analog for the AE cases obtained by numerical comparison of their fluctuation measures $P(s)$ and Σ_2 . The third column in the table contains the values of $\Sigma_2(r)/r$ at $r = 20$ for each AE case (see figure 4) and the fifth column shows the $\chi = \lim_{r \rightarrow \infty} \Sigma_2(r)/r$ value expected by the analytical formula $\chi = \frac{4\gamma c}{\beta\pi}$ based on AE-BE analogy.

Case	β	Σ_2/r	C	$\chi = \frac{4\gamma c}{\beta\pi}$
AE_1	1	0.03	0.12	0.08
AE_2	1	0.1 – 0.2	0.3	0.38
AE_4	2	0.03	0.07	0.04
AE_5	2	0.3	0.3	0.38

Figure 1

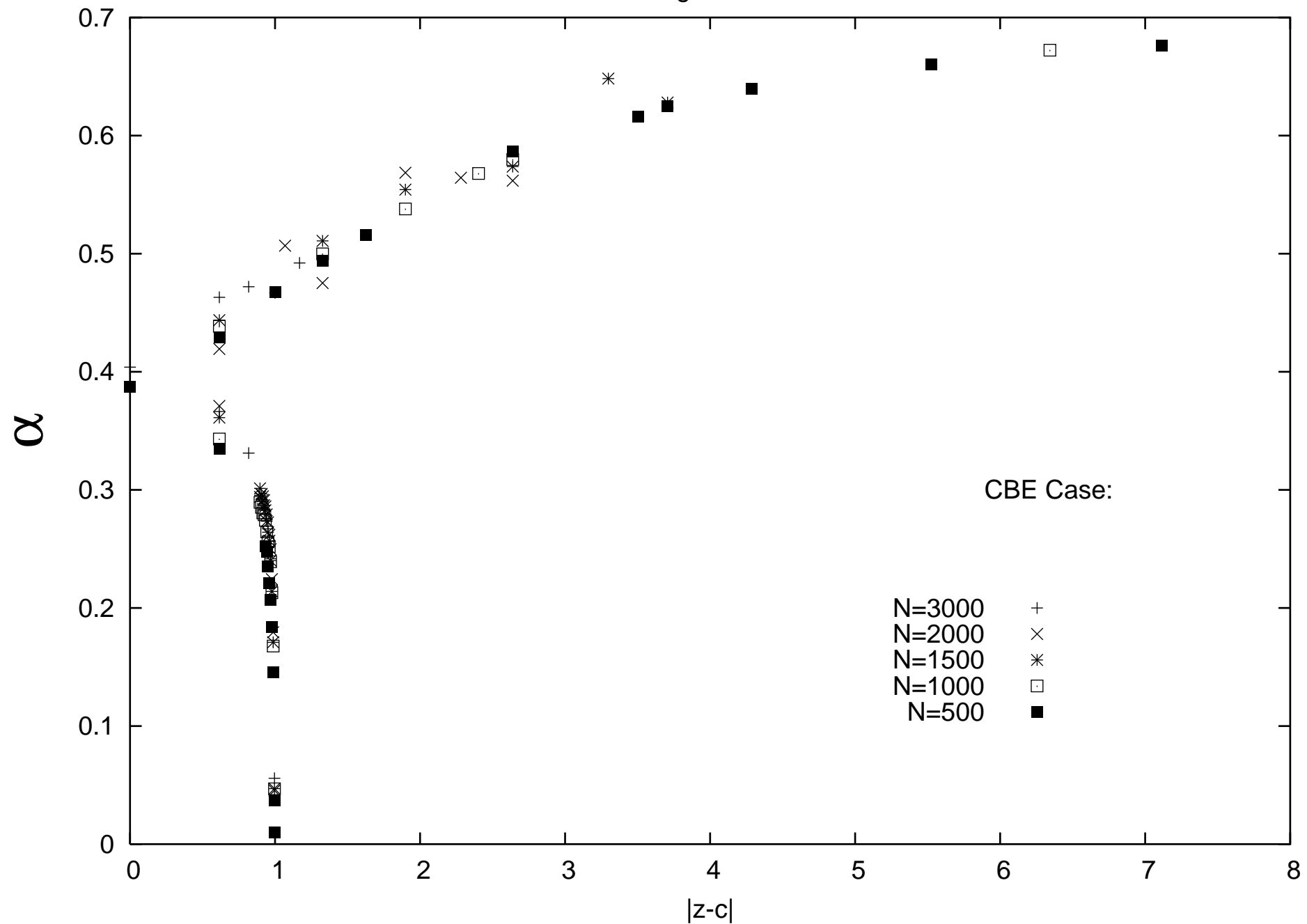


Figure 2(a)

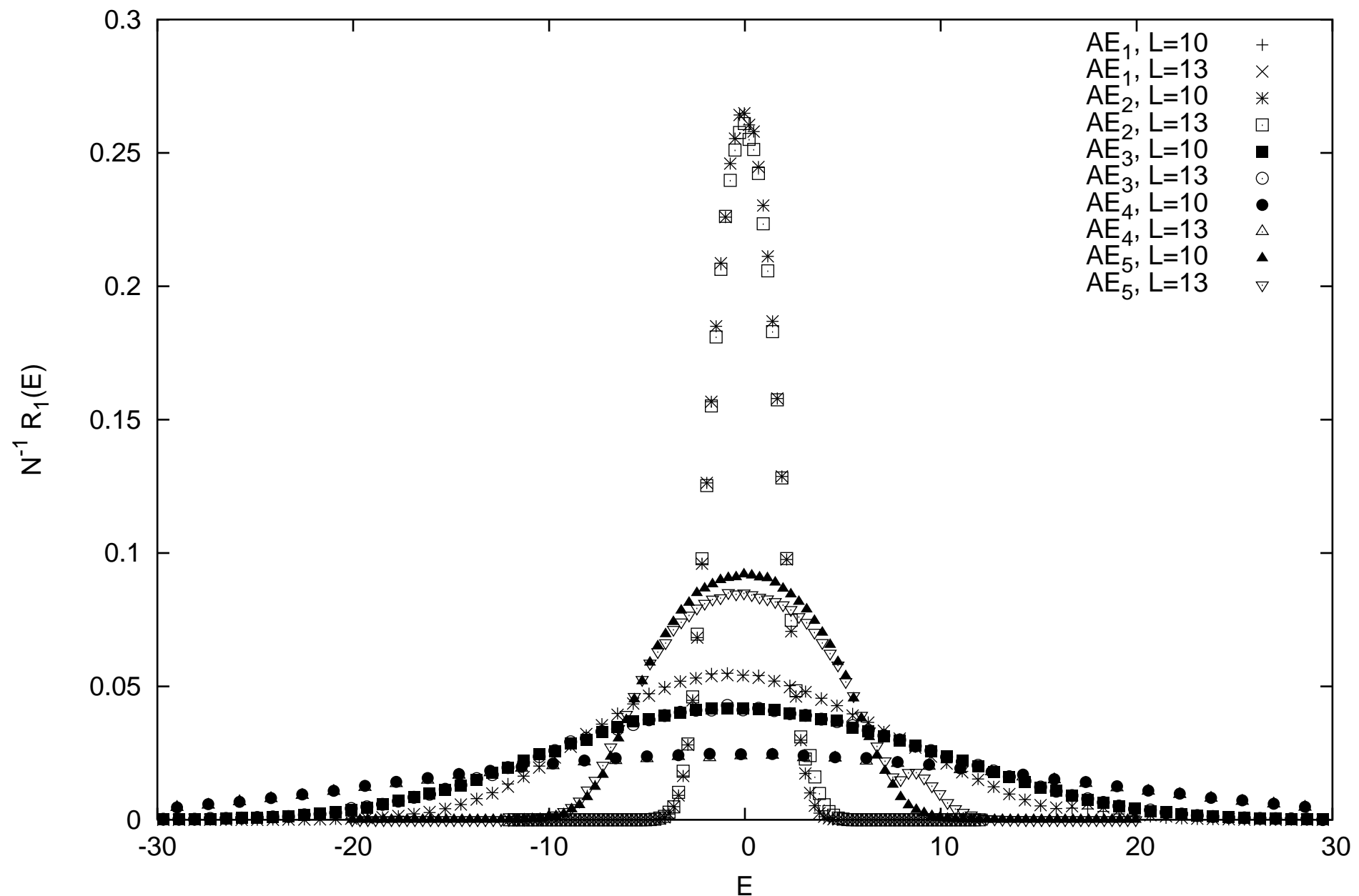


Figure 2(b)

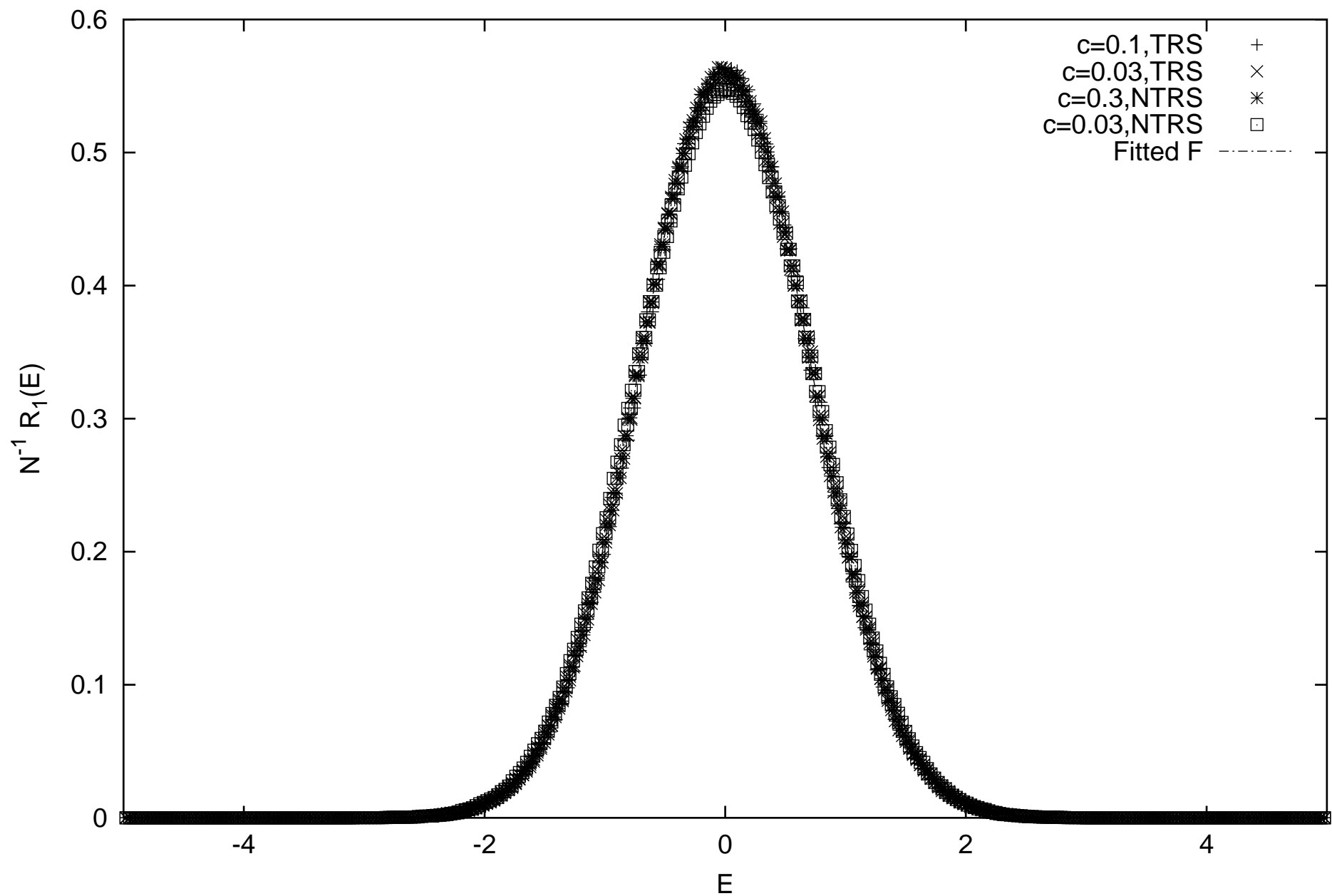


Figure 3(a)

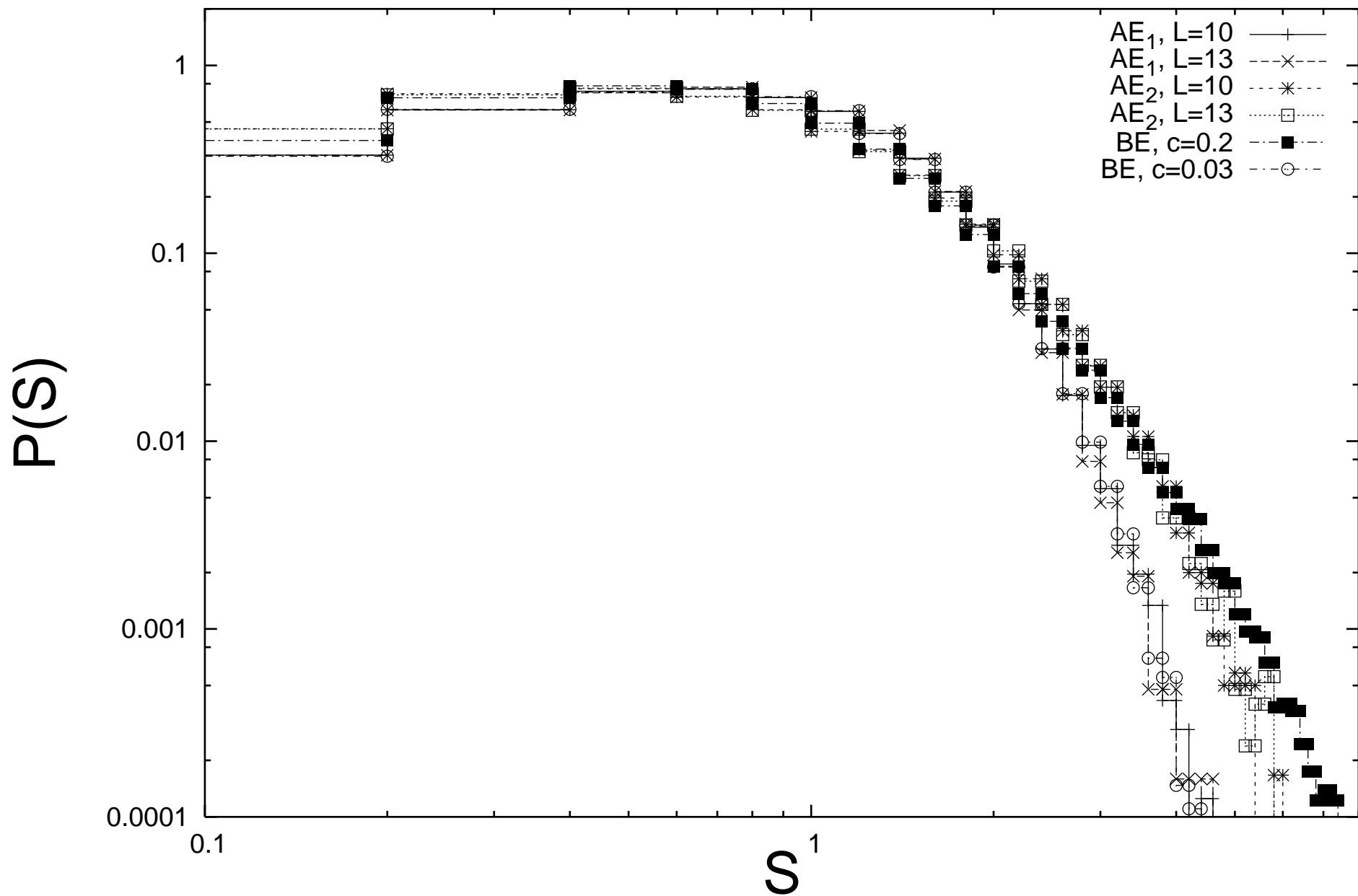


Figure 3(b)

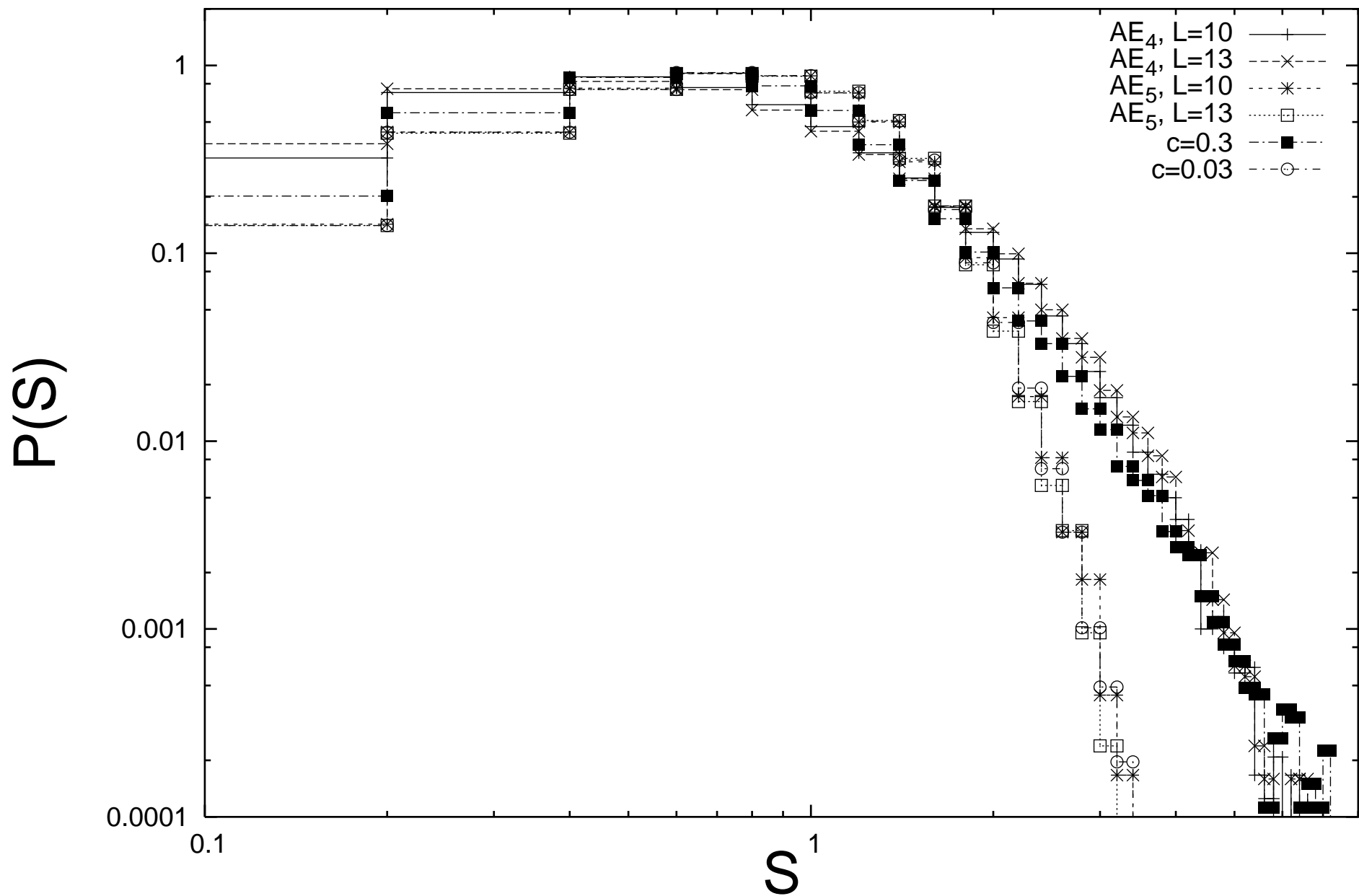


Figure 4(a)

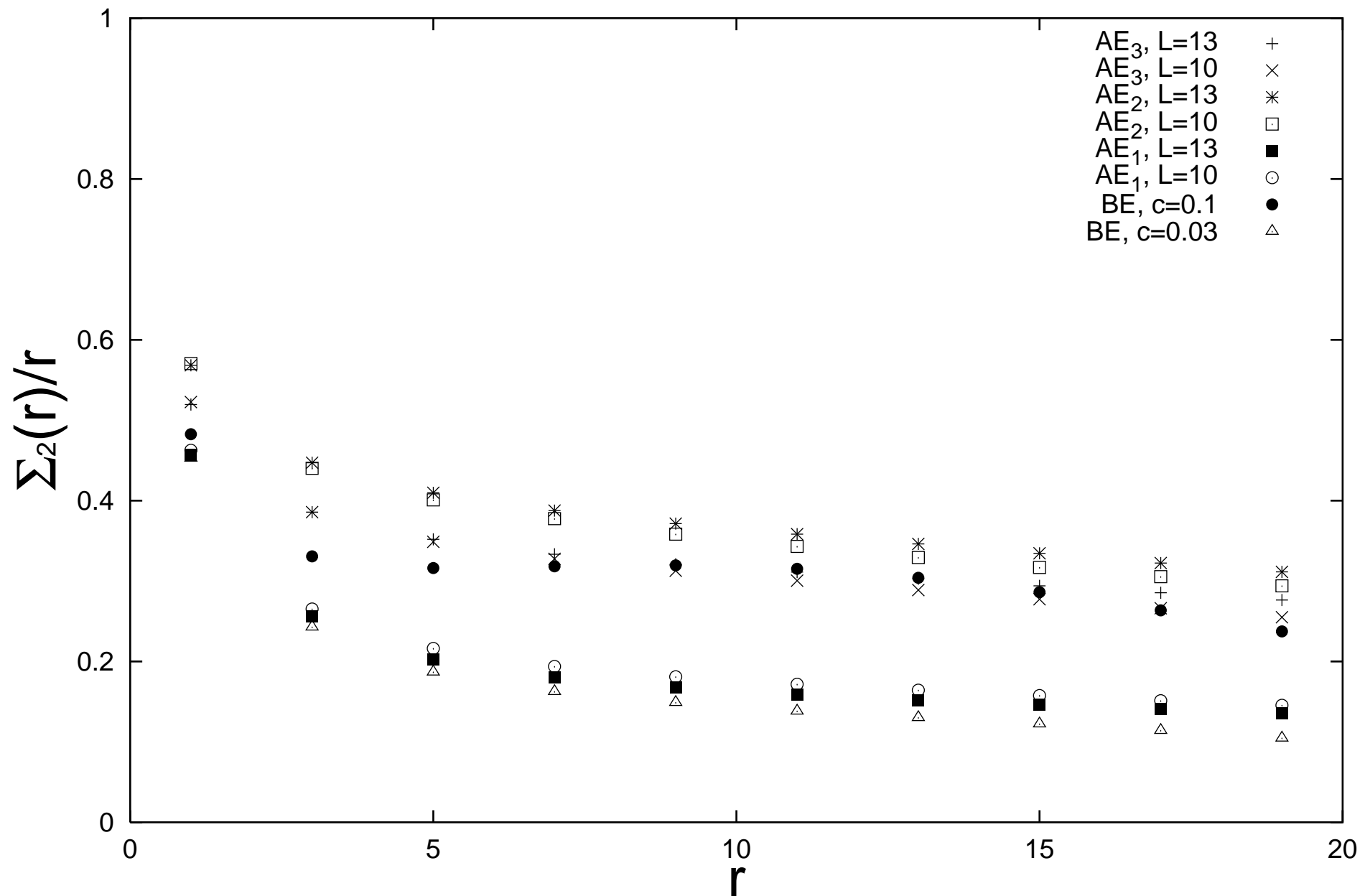


Figure 4(b)

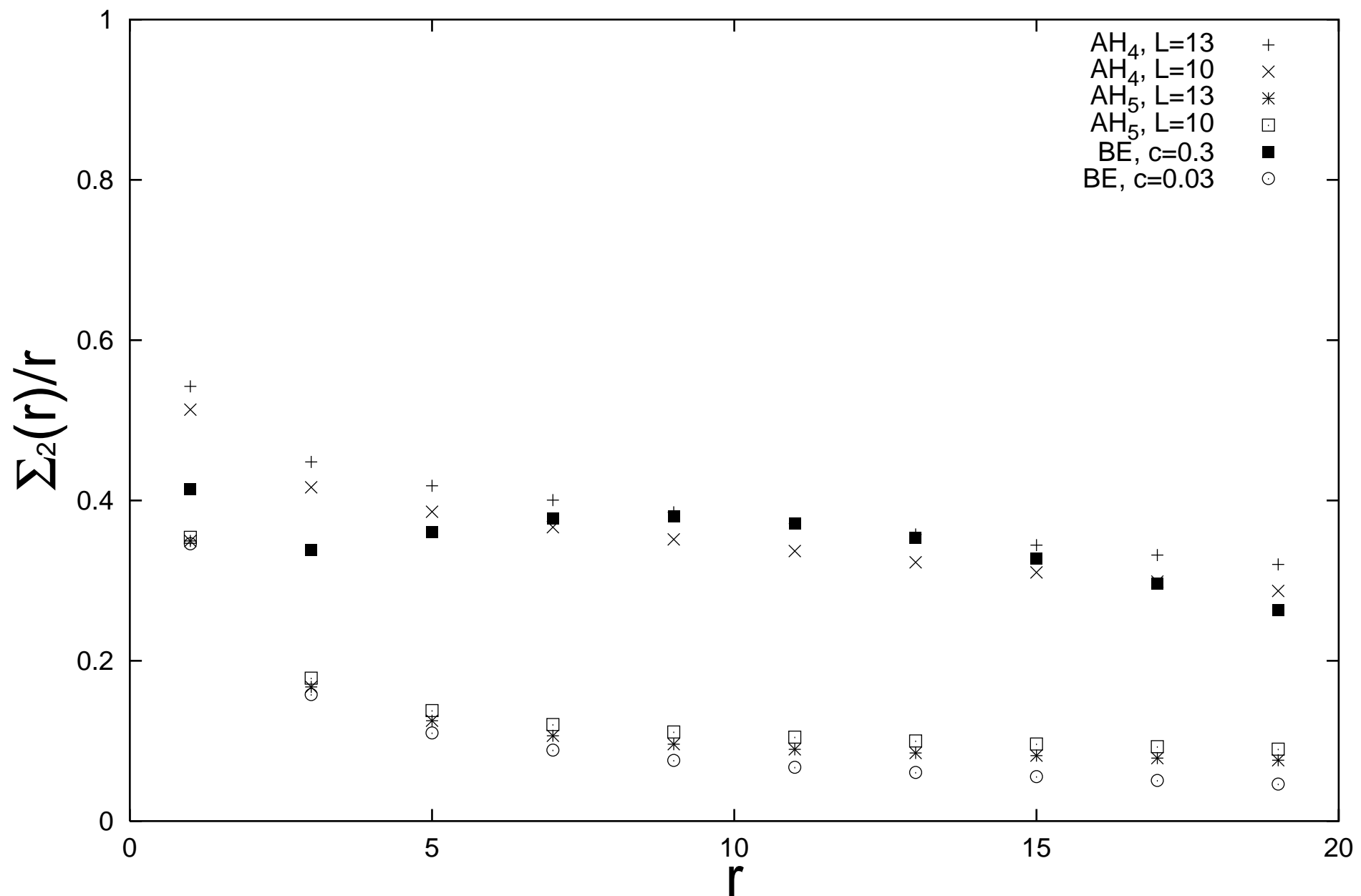


Figure 5

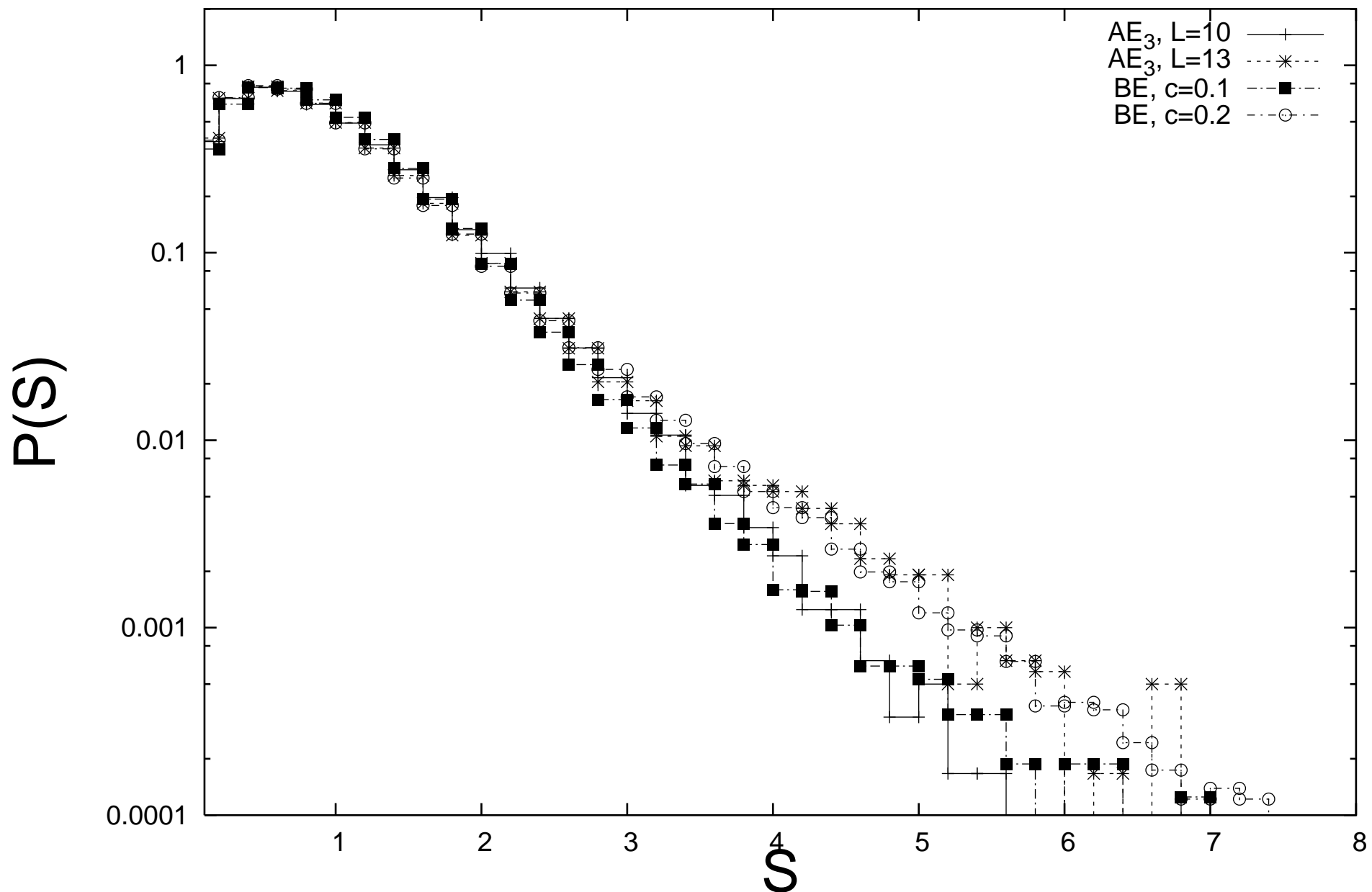


Figure 6

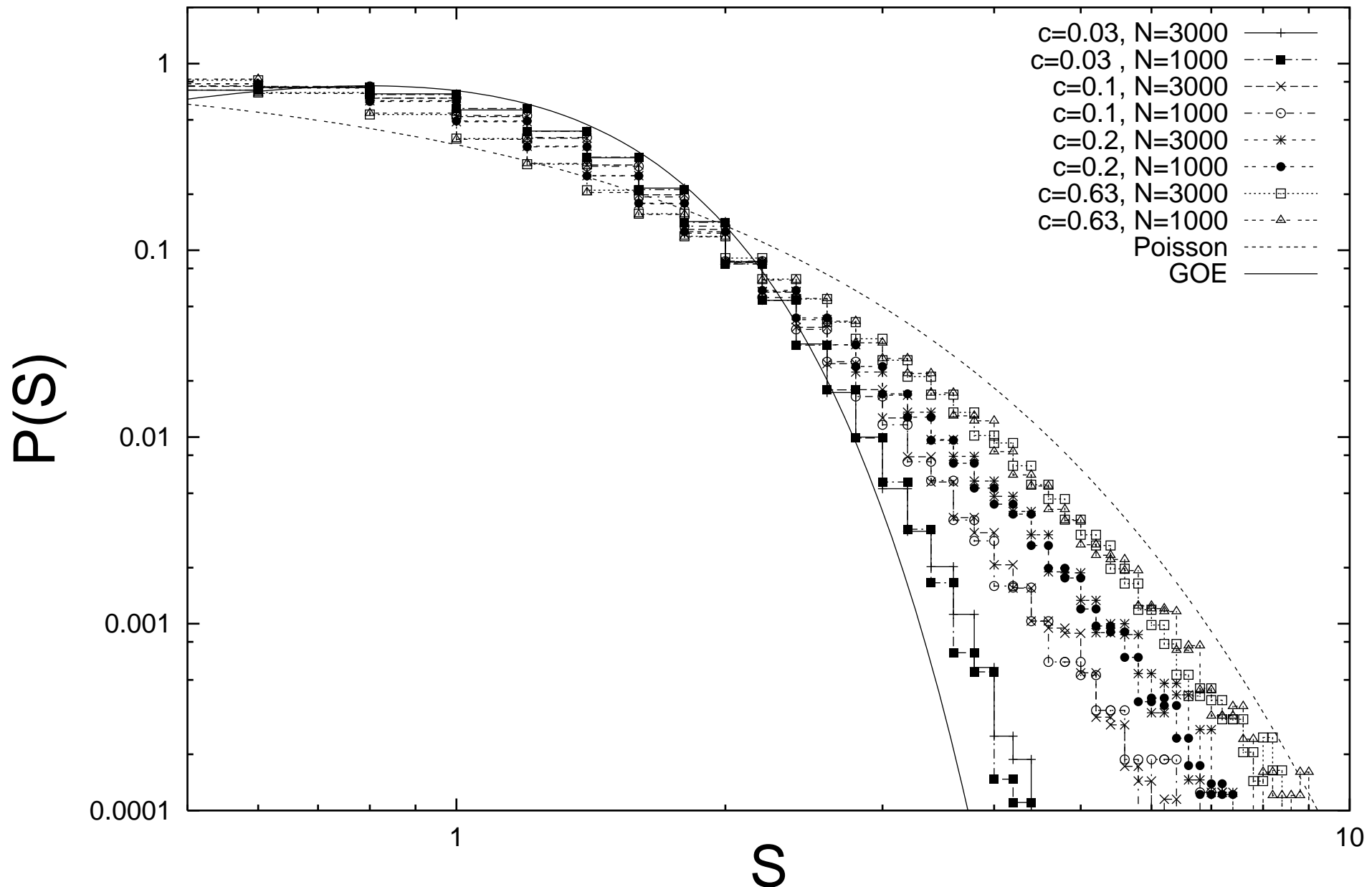


Figure 7

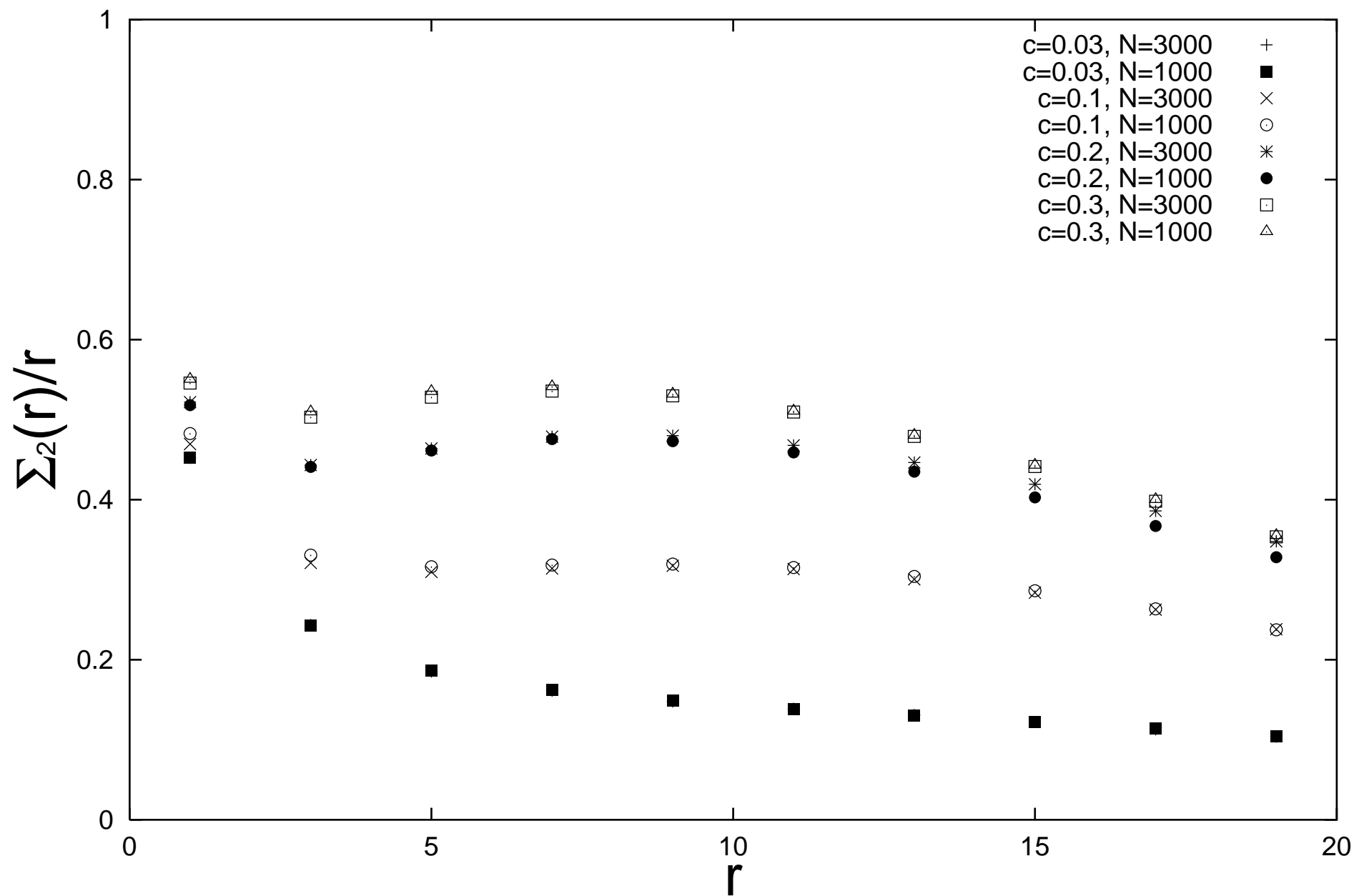


Figure 8

